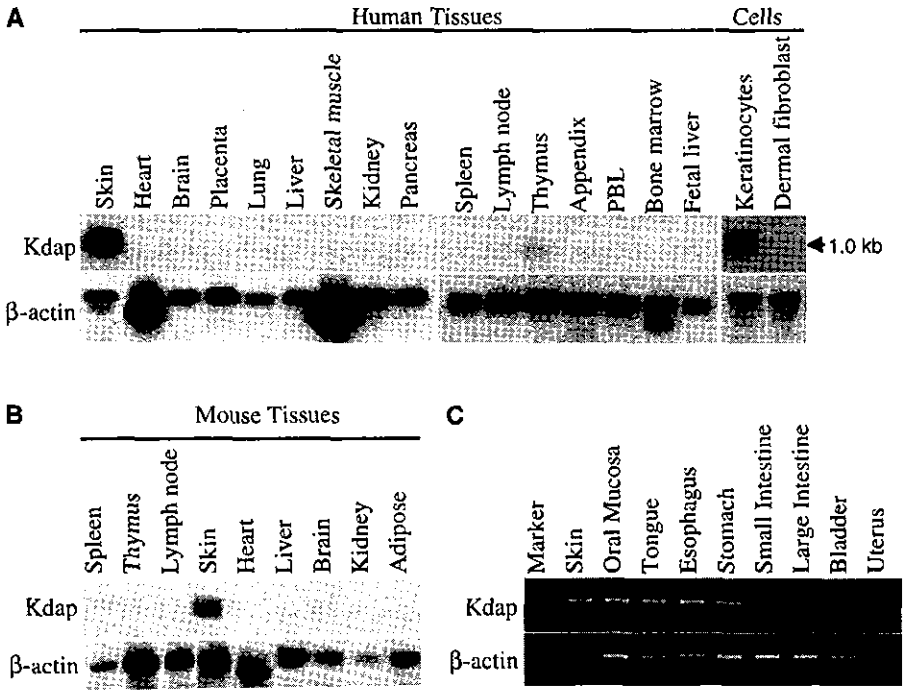

Figure 2
mRNA expression of human and mouse keratinocyte differentiation-associated protein (Kdap). mRNA isolated from primary-cultured cells and various human (*A*) and mouse (*B*) tissues was examined by *northern blotting for mRNA expression of* Kdap or β-actin. Expression was also assayed using RT-PCR of RNA isolated from different mouse epithelial tissues using RT-PCR (*C*).

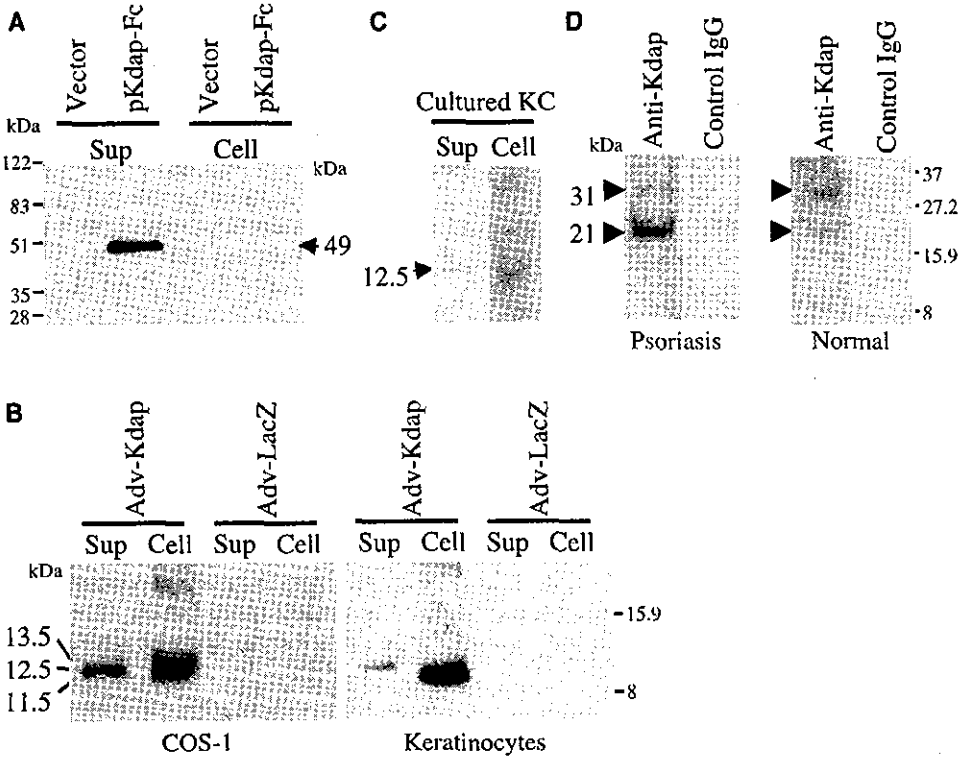

Figure 3
Protein expression of human keratinocyte differentiation-associated protein (Kdap). *Human Kdap protein was characterized by western* blotting of culture supernatant and protein extracts prepared from Kdap gene-transfected cells, primary-cultured keratinocytes, psoriatic or normal scales. (*A*) COS-1 cells were transfected with an empty vector (Vector) or an expression vector (pKdap-Fc) encoding for a fusion protein of the entire sequence of human Kdap (including a signal sequence) and Fc portion of immunoglobulin. At 2 d post-transfection, the culture supernatant (Sup) was harvested and whole-cell extracts (*Cell*) were prepared. *Aliquots (10% each fraction)* were subjected to SDS-PAGE analysis followed by western blotting, using anti-human IgG Ab. (*B*) COS-1 cells (*left panel*) or keratinocytes (*right panel*) were infected with recombinant Adv encoding Kdap (Adv-Kdap) or LacZ gene (Adv-LacZ). Likewise, the small aliquots (5% and 10% for COS-1 cells and keratinocytes, respectively) were examined for expression of Kdap protein. (*C*) Whole-cell extracts were prepared from primary-cultured keratinocytes and the supernatant was harvested and concentrated *10–20-fold. Small aliquots* (10% each) were applied for SDS-PAGE. (*D*) Crude extracts (75 μg) prepared from scales psoriatic or normal scales were assayed by western blotting, using anti-human Kdap Ab or control rabbit IgG.

kDa in the extracellular fraction and two bands (13.5 and 11.5 kDa) in the intracellular fraction (no bands were detected with control Ab). The latter bands most likely correspond to a precursor containing SS and the mature form, respectively. Ab specificity was confirmed by the absence of detectable bands in the two fractions of COS-1 cells infected with Adv-LacZ (expression vector for β-galactosidase gene). We noted the extracellular mature form (12.5 kDa) to be slightly larger than the intracellular mature form (11.5 kDa); both mature forms were markedly larger than the size predicted from the primary amino acid sequence (8.7 kDa). Similar differences in molecular weights were also detected using Adv-infected keratinocytes (Fig 3*B*). Kdap protein was found mostly in the intracellular fraction, although lower levels were detected in the supernatant, indicating that secretion was blocked partially in these infected keratinocytes. This low secretion may be due to lack of mature lamellar granules (secretory vesicles) in *in vitro* cultured keratinocytes (undifferentiated phenotype). In primary-cultured keratinocytes in which Kdap is synthesized from the endogenous gene (rather than from the transgene), only small amounts of protein were detected in both extracellular and intracellular fractions when more proteins and longer exposure to an X-ray film were involved (Fig 3*C*). Nonetheless, secretion of Kdap was proved by cleavage of N-terminal sequence and detection of Kdap protein in culture supernatants of transfected (transgene expression) and non-transfected keratinocytes (endogenous gene expression).

We also examined protein expression of Kdap in crude extracts prepared from scales of psoriatic or normal skin (not cultured cells) (Fig 3*D*). Western blotting using the same Ab detected two bands in the extracts of psoriatic scales: a thicker band (21 kDa) and a thinner band (31 kDa). These molecular weights were about two to three times larger than the 11.5 kDa detected in the cell extracts of non-transfected and transfected keratinocytes (Fig 3*B*). In normal scales, both bands were also detected, but expression levels were much lower than in psoriatic scales, suggesting upregulated expression of Kdap *in situ* in psoriatic skin. Moreover, the ratio of the two bands' intensities was converse to that found in psoriatic scales. Variations in the molecular weight of the secreted (matured) Kdap protein were not detected. By contrast, intracellular Kdap appears to vary, most likely due to post-translational modification.

***In situ* expression in human skin** Using the previous Ab, we examined Kdap expression in normal human skin. Indirect immunofluorescence highlighted the upper spinous and granular layers on control cryostat sections of the human epidermis (see arrows in Fig 4*A*). Staining was predominantly observed in an alternate wave-like pattern, with the strongest staining at the apical edges of the granular cells (inset in Fig 4*A*). There was little or no staining of the cornified layer and very weak staining was occasionally seen in the mid-epidermal layers. By contrast, in lesional skin of psoriatic patients, Kdap was expressed more widely and at high levels throughout suprabasal keratinocytes (Fig 4*B*). This expression pattern in psoriasis is similar to that reported for SKALP/elafin (Pfundt *et al*, 1996) and for cystatin M/E (Zeeuwen *et al*, 2001), both of which are low-molecular-weight and secreted proteins with anti-proteinase activity. It should be noted that this more widespread Kdap expression in psoriasis was not seen in other cornification disorders, such as the bullous and non-bullous types of congenital ichthyosiform erythroderma, lamellar ichthyosis with or without TGM1 mutation, and palmoplantar keratoderma.

We next examined Kdap mRNA expression in normal skin using *in situ* hybridization (Fig 4*C*). Unlike its protein expression, Kdap mRNA was detected more widely throughout suprabasal keratinocytes. This difference between protein and mRNA expression is reminiscent of involucrin, an established marker of keratinocyte differentiation (de Viragh *et al*, 1994). Consistent with the protein expression, Kdap was not expressed by basal keratinocytes, strongly suggesting that Kdap is also a marker of keratinocyte differentiation.

Kdap is secreted into the extracellular space via lamellar granules To determine the ultrastructural localization of Kdap in granular keratinocytes, we conducted immunoelectron microscopic analysis of normal human epidermis stained with anti-Kdap Ab and gold particle-conjugated anti-rabbit IgG (Fig 5). Kdap staining localized to areas immediately beneath the apical side of the keratinocyte

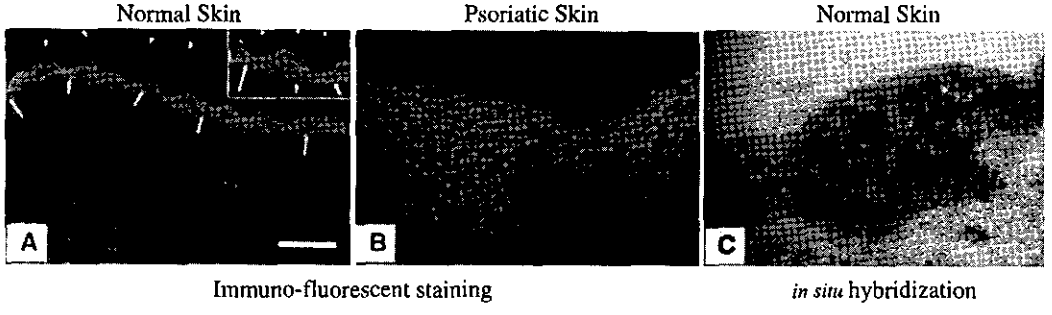

Figure 4
Keratinocyte differentiation-associated protein (Kdap) expression in normal and psoriatic skin. Frozen skin sections prepared from normal healthy adults (*A*, *C*) and psoriatic patients (*B*) were immunofluorescently stained with anti-Kdap Ab and fluorescein isothiocyanate-conjugated anti-rabbit Ab (*A*, *B*) or hybridized *in situ* with anti-sense RNA probe for the Kdap gene (*C*). A higher magnification is provided in inset (*A*). The granular layer and stratum corneum are indicated by arrows and arrowheads, respectively (*scale bar*: 50 mm). No staining was observed with control rabbit IgG or sense RNA probe. Data shown are representative of staining of skin biopsies from three individuals with psoriasis.

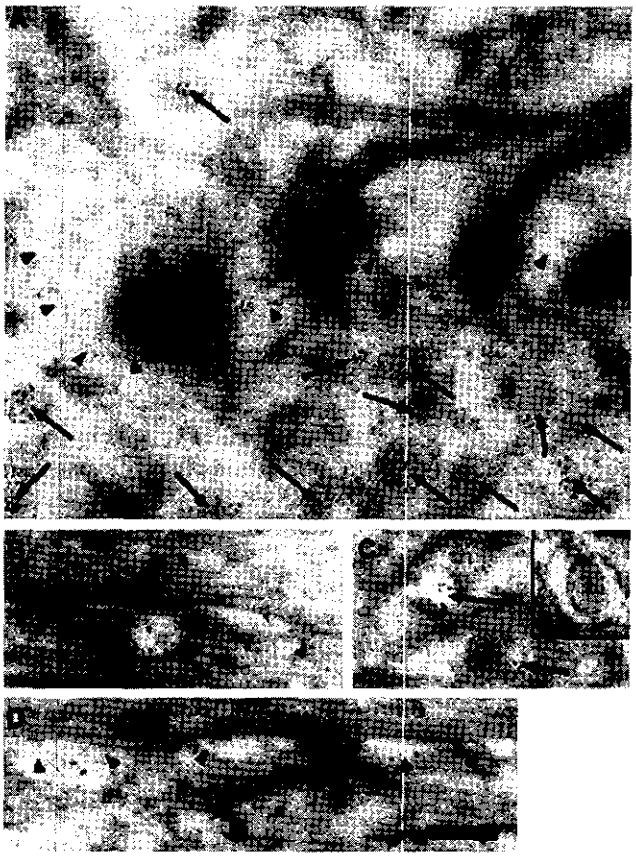

Figure 5
Keratinocyte differentiation-associated protein (Kdap) protein is localized to lamellar granules of keratinocytes. After staining normal skin with anti-Kdap Ab and secondary Ab conjugated with gold particles, localization of Kdap protein ultrastructually was examined in the granular keratinocytes. (*A*) Low magnification: immuno-gold label (representing Kdap) was found in small vesicles under the apical plasma membrane of granular keratinocytes (*arrows*), a localization similar to that of lamellar granules. Some labeled granules were also seen fusing with or in close association to the plasma membrane. (*B*) Kdap was also present in the intercellular space. (*C*) Higher magnification: although membrane-bound vesicles failed to show the classic lamellar characteristics of membrane coating granules seen in routine transmission EM sections, the size and frame structure were identical to those of lamellar granules (inset). Multiple clusters of lamellar granule-like vesicles were localized within elongated, electron-lucent areas of the cytoplasm just under the plasma membrane (*arrows*). (*D*) Kdap was observed close to or on the cell membrane (*arrowheads*) of granular keratinocytes (*scale bars*: 2a 50 nm, 2b, c and d 100 nm).

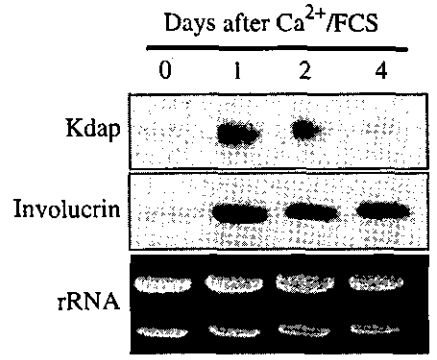

Figure 6
Expression of keratinocyte differentiation-associated protein (Kdap) mRNA is markedly induced during *in vitro* keratinocyte differentiation. At indicated time points after inducing differentiation with high-dose Ca^{2+}, total RNA was isolated from treated cells and examined by northern blotting for Kdap and involucrin mRNA expression. Amounts of ribosomal RNA (rRNA) detected by ethidium bromide staining were similar in all four RNA samples.

plasma membrane in the upper suprabasal and granular layers (Fig 5). These areas were rich in apparently membrane bound vesicles containing both variably electron dense material that was consistent with them being membrane-coating granules (lamellar granules). These granules could sometimes be seen closely arranged together in a distinctive pattern beneath the plasma membrane. By contrast, there were very few Kdap-labeled vesicles in the region directly above the plasma membrane (Fig 5*A*). The position of the labeling was over both the vesicle plasma membrane and the center of the vesicle (Fig 5*A–C*). The morphology of the cryofixed and substituted control skin often, but not always, failed to reveal the fine detail of the membrane coating (lamellar) granules as seen by conventional EM (Fig 5*C*). Both the size of the vesicles stained by anti-Kdap Ab and their distribution pattern within granular keratinocytes strongly suggests that Kdap is in the lamellar granules or their contents. The Kdap-containing granules were seen close to the plasma membrane, and Kdap staining was also observed in the intercellular space (Fig 5*B* and *D*). Morphometric analysis of Kdap labeling (>750 gold particles) at the outer surface of the plasma membrane in the upper granular keratinocyte layers showed a significant proportion (40%) of labeling on or between the external surfaces of the plasma membrane or between granular cells in the intercellular spaces (the majority of the remaining 60% of plasma membrane labeling was restricted to the lamellar granules subjacent to the apical plasma membrane (Fig 5*B* and *D*). These results indicate that Kdap is secreted by differentiated keratinocytes and may be incorporated into the lipid layer and the external surface of the CCE.

Kdap mRNA expression is upregulated markedly during keratinocyte differentiation *in vitro* To examine the effect of keratinocyte differentiation on Kdap mRNA expression, we cultured keratinocytes in low-Ca^{2+} media to maintain these cells in a basal state, and then induced differentiation by shifting to high-Ca^{2+} media containing 10% FCS. Time-dependent changes in mRNA expression were assessed by northern blotting, and keratinocyte differentiation was monitored in parallel by involucrin mRNA expression. In low-Ca^{2+} media, both Kdap and involucrin were expressed at background levels (Fig 6). After shifting to high-Ca^{2+} media, involucrin mRNA was increased markedly after 24 h and this high level was maintained for 4 d. Kdap mRNA was also upregulated at 24 h (60-fold higher than in untreated keratinocytes), but unlike involucrin, Kdap's upregulated expression lasted for only 2 d. These results indicate that Kdap (like involucrin) is a marker of keratinocyte differentiation; however, Kdap and invlucrin differ in the kinetics of mRNA expression during differentiation *in vitro*.

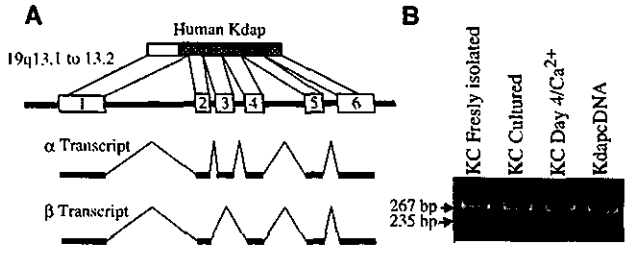

Figure 7
Human β transcript is generated by alternative splicing mechanisms. (*A*) The organization of human keratinocyte differentiation-associated protein (Kdap) gene on chromosome 19q13.1 to 13.2 is represented schematically. The nucleotide sequence of α transcript (a full-length form) segmented into six exons, and aligned to that of β transcript with deletion of exon 3. (*B*) Total RNA was isolated from keratinocytes that were freshly isolated from neonatal foreskin tissue, primary cultured, or treated with high Ca^{2+} medium (day 4). RNA was examined for mRNA expression of α and β transcripts by RT-PCR using a primer set (Materials and Methods). Full-length Kdap cDNA was also PCR amplified as control. PCR products were then size-fractionated through 8% native PAGE and stained with ethidium bromide.

A spliced variant is produced by alternative splicing mechanisms In isolating a full-length cDNA clone for Kdap (α transcript), we identified an additional cDNA clone containing a shorter insert (termed β transcript) (Fig 7*A*). Nucleotide sequence analysis showed that the coding sequence of the β transcript is identical to an alternatively spliced form (GenBank accession number AA58342) that was reported by Oomizu *et al*. Note, however, that the two transcripts differ in their 3′-untranslated region. Amino acid sequence deduced from the DNA sequences revealed a deletion of amino acid 43–56. We also examined expression levels of β transcript relative to a transcript in keratinocytes by RT-PCR using a primer set designed to amplify a 267 bp fragment for a transcript and a 235 bp for β transcript (Fig 7*B*). In addition to a 267 bp fragment, a band corresponding to a 235 bp was noted. This band was very faint in PCR products of RNA from keratinocytes freshly isolated from skin, and was unchanged in primary-cultured keratinocytes induced to differentiate after treatment with high-Ca^{2+} media. These results show that the spliced variant of Kdap mRNA is not the major transcript in keratinocytes.

To determine whether this spliced variant was generated by alternative splicing mechanisms, we searched for the Kdap gene in the human genome database (provided by NCBI). An entire sequence of Kdap cDNA segmented into six exons was found in the locus between 13.1 and 13.2 on chromosome 19 (Fig 7*A*): exon 1 encoded for the SS and a part of N-terminal mature Kdap; and other five exons encoded for the rest of the amino acid residues. The 5′- and 3′-flanking sequences of each exon contained conserved splice acceptor/donor sequences. A nucleotide sequence missing from the β transcript was identical to exon 3, indicating that the β transcript was generated by alternative splicing (exon skipping).

Discussion

Kdap was first identified by Oomizu *et al* (2000) by suppression subtractive cDNA cloning of skin from rats at different embryonal stages of hair differentiation (prehair-germ *vs* hair-germ stages). They also identified mouse and human homologs and their spliced variants. Expression studies in rat showed that: (1) Kdap mRNA was induced after the hair-germ stage (quantitative RT-PCR); (2) its expression was restricted to epithelial tissues in rat embryo tissues (RT-PCR); and (3) skin expression was confined to the suprabasal layers of embryonal epidermis (*in situ* hybridization).

At the time we initiated our studies, Kdap was not registered in the GenBank database nor were Oomizu's results published. Employing a different strategy, we coupled an SS trap with differential colony hybridization and isolated the same gene from a cDNA library constructed with mRNA from primary-cultured human keratinocytes. Using a wide spectrum of human and mouse tissues and northern blotting, we affirmed the epithelium-specific expression of Kdap and its suprabasal layer-specific expression within the epidermis. We did note the new finding of low-level expression by human thymus (Figs 2 and 4*C*).

Expanding on the findings of Oomizu *et al* we found that: (1) human Kdap is secreted by keratinocytes (N-terminal amino acid sequence functioned as an SS; Kdap protein was detected in the extracellular fraction of transfected and non-transfected keratinocytes (Fig 3); and it resided in lamellar granules of granular keratinocytes and the intercellular space of the stratum corneum (Fig 5); (2) Kdap protein is confined to the granular layer of normal epidermis (which is not identical to its mRNA expression pattern); (3) expression in psoriatic skin is more diffuse, involving suprabasal layers; (4) mRNA expression is regulated by keratinocyte differentiation; and (5) spliced variant is produced by alternative splicing mechanisms and expressed in keratinocytes only at very low levels (in contrast to the full-length form).

We observed variation in the molecular weight of Kdap protein. The molecular weight of Kdap produced by transfected cells was larger than that predicted from the primary amino acid sequence (Fig 3*B*). This is due most likely to post-translational modification in which fatty acids, glycosylphosphatidylinositol (GPI) (Chatterjee and Mayor, 2001), or other small sized molecules are incorporated. Glycosylation may not take place because *Kdap* contains neither possible *N*-glycosylation sites nor putative *O*-glycosylation sites (e.g., proline-, serine-, threonine-rich regions) (Wilson *et al*, 1991). We also observed another type of modification. The molecular weight of Kdap in crude extracts from psoriatic and normal skin was two to three times larger than that detected in transfected and non-transfected keratinocytes (Fig 3*C*). This finding suggests that Kdap is polymerized or cross-linked to polymerized proteins in the skin. Because polymerization was not found in the extracellular Kdap proteins, we speculate that Kdap is anchored to structural proteins by TGase inside keratinocytes, as has been shown for elafin and cystatins (Zeeuwen *et al*, 2001; Nakane *et al*, 2002). But we could not document TGase-dependent cross-linking of Kdap (data not shown), which may mean that Kdap polymerization is achieved by other mechanisms.

Since highly polymerized Kdap cannot be solubilized using our buffer containing Triton X-100 detergent, we may have lost the majority of Kdap protein during protein

extraction. This possibility may thus account for poor expression of Kdap (in western blotting) in intracellular fractions of non-transfected primary-cultured keratinocytes (Fig 3C) and also explain the poor efficiency of secretion by keratinocytes.

Recent molecular studies on CCE components have documented the presence of low-molecular-weight secreted proteins in the protein envelope consisting of an insoluble complex of proteins, which include SKALP/elafin (Schalkwijk *et al*, 1990; Wiedow *et al*, 1990), secretory leukocyte proteinase inhibitor (SLPI) (Jin *et al*, 1997), lympho-epithelial Kazal-type-related inhibitor (LEKTI) (Mägert *et al*, 2001) cystatin A and M/E (Takahashi *et al*, 1992; Sotiropoulou *et al*, 1997a,b; Zeeuwen *et al*, 2001), plasminogen activator inhibitor-type 2 (PAI-2) (Lavker *et al*, 1998), and bikunin (Cui *et al*, 1999). All these proteins possess activity to inhibit either serine or cysteine proteinases, some of which are further characterized by restricted expression to keratinocytes. These inhibitors have been proposed to play a pivotal role in regulating renewal of the epidermis and protecting the epidermis from tissue damages by suppressing activities of endogenous and exogenous proteinases.

Kdap shares some attributes with these epidermal proteinase inhibitors, including being a low-molecular-weight secreted protein and showing a restricted expression to granular keratinocytes (or CCE). By contrast, Kdap appears unique with respect to its localization within lamellar granules and the existence of naturally occurring spliced variants producing truncated isoforms. In addition, Kdap might be efficiently secreted by granular keratinocytes (Fig 5), suggesting that it may function as a soluble regulator in the extracellular space.

Because of the similarities to epidermal proteinase inhibitors, we hypothesized that Kdap possesses activity to inhibit proteinase and/or growth of microbes. Purified His-Kdap and His-DHFR were used to determine whether Kdap could inhibit the activity of cysteine proteinases (papain, ficin, and cathepsin B) and serine proteinases (chymotrypsin and trypsin). His-Kdap (10 μM) inhibited the proteinase activity of papain (100 nM) almost completely, whereas His-DHFR at the same concentration failed to do so (data not shown). Although we found anti-proteinase activity of Kdap, the activity appears 10–100-fold lower than those for other epidermal inhibitors (e.g., cystatin M/E; Sotiropoulou *et al*, 1997). Secondly, His-Kdap was assayed for activity to suppress the growth of microbes (*Streptococcus group A*, *E. coli*, *Staphylococcus aureus*, and *Candida albicans*). No suppressive activity was found with any of the microbes tested. Kdap is thus likely to possess disparate function from other low-molecular-weight secreted proteins in the CCE, although there remains the possibility that post-translational modification is required to activate Kdap function (His-Kdap produced in *E. coli* assumed to have no modification similar to that in keratinocytes).

Materials and Methods

Cell culture Primary keratinocytes and dermal fibroblasts were isolated, respectively, from epidermis and dermis of newborn human foreskins as described before (Girolomoni *et al*, 2000). Isolated keratinocytes were maintained and expanded in keratinocyte-SFM media (Invitrogen, Carlsbad, California). Third- to sixth-passaged keratinocytes (60%–80% confluency) served as a source of RNA for cDNA library construction and for experiments examining gene expression. Dermal fibroblasts and COS-1 cells were cultured in Dulbecco's modified Eagle's medium (DMEM) supplemented with 10% fetal calf serum (FCS).

Cloning of keratinocyte-specific and SS-encoding genes For the SS trap, we constructed a cDNA library based on a report by Tashiro *et al* (1997). We fused 5′-end cDNA sequences from keratinocyte mRNA in frame to the gene for a variant human interleukin-2 receptor α (hIL-2Rα) lacking SS in order to produce hIL-2Rα fusion proteins. Eight thousand independent colonies were sorted randomly from the library into 163 pools (49 clones per pool) for SS trap screening (Tashiro *et al*, 1997; Bonkobara *et al*, 2003). Plasmid DNA (0.2 μg) from each pool (all colonies in a group) was transfected into COS-1 cells (1×10^4) seeded on eight-well chamber slides (NUNC, Naperville, Illinois) using FuGENE 6 (Roche Molecular Biochemicals, Indianapolis, Indiana). After 3 d of culture, the transfectants were assayed by immunocytochemistry for surface expression of hIL-2Rα; fixed cells were incubated with 0.5 μg per mL of mouse monoclonal antibody (mAb) against hIL-2Rα (R&D Systems Inc., Minneapolis, Minnesota). After incubation with biotinylated anti-mouse IgG, avidin-peroxidase and 3-amino-9-ethylcarbazole (AEC) (DAKO, Carpinteria, California) were applied and the color stain was examined under light microscopy. Pools showing surface expression of IL-2Rα were sub-divided (7 clones per subpool), and then screened further in the above manner. Finally, cDNA clones in positive subpools were examined clonally for IL-2Rα surface expression.

cDNA clones with IL-2Rα surface expression were screened by differential hybridization as described previously (Ariizumi *et al*, 1997, 2000) for cDNA expressed selectively by keratinocytes. Selected colonies (193 clones) were transferred to nylon membranes and hybridized with total cDNA probes prepared from poly(A)$^+$ RNA of keratinocytes or with total cDNA probes of dermal fibroblasts. This differential hybridization led to selection of 36 cDNA clones with strong hybridization signals for keratinocyte total cDNA probes, but little or no signals for dermal fibroblast probes.

The SS-trapped cDNA clones expressed selectively by keratinocytes were examined for nucleotide sequence identities in GenBank and EST databases using a Blast search program from the National Center for Biotechnology Information (NCBI). cDNA clones found in the EST database were evaluated for full-length nucleotide sequences (SS-trapped cDNA clones contain 5′-end sequences only) using 3′ rapid amplification of cDNA ends (3′ RACE) system (Invitrogen). The clones with longest cDNA inserts were selected and their nucleotide sequences were determined.

Northern blotting and RT-PCR analysis Northern blotting was performed as described previously (Ariizumi *et al*, 1995). Poly(A)$^+$ RNA (2 μg) isolated from primary-cultured human keratinocytes, dermal fibroblasts, foreskins, and mouse organs were size-fractionated on a vertical agarose gel, transferred electrophoretically onto a nylon membrane, and hybridized in buffer containing 1×10^6 c.p.m. per mL of ^{32}P-labeled cDNA for Kdap or β-actin gene. After incubating for 16 h at 42°C, membranes were washed and autoradiographed. For tissue distribution of human Kdap mRNA, a nylon membrane (Human Multiple Tissue Blots purchased from BD Biosciences, Palo Alto, California) with an array of mRNA (2 μg) isolated from various human organs was hybridized according to the manufacturer's recommendations.

To determine Kdap gene expression in total RNA isolated from mouse epithelial tissues, RT-PCR was performed (Ariizumi *et al*, 1995). RNA (100 ng) was reverse-transcribed and then PCR-amplified in one tube (50 μL) containing 0.2 mM dNTP, 1.2 mM

$MgCl_2$, 20 pmol primers, and SuperScript II RT/Taq mix (Superscript One-Step RT-PCR System, Invitrogen) using a protocol for cDNA synthesis (45°C for 30 min, and then at 94°C for 2 min). The PCR cycling protocol included incubation at: 94°C for denaturation (45 s); 60°C for mouse Kdap or 55°C for β-actin primers for annealing (45 s); 72°C for extension (60 s); and 30 cycles. PCR products (20 μL) were size-fractionated electrophoretically on 1.2% agarose gel and visualized by ethidium bromide staining. The following primers were used to PCR-amplify cDNA: for mouse Kdap, 5′-CAGCCCAAACCGGACACCAT-3′ and 5′-GGGGAACTGAGGCAAGGAAGATTT-3′; and for mouse β-actin, 5′-GAGCGGGAAATCGTGC GTGACATT-3′ and 5′-GAAGGTAGTTTCGTGGATGCC-3′.

For experiments examining the expression of alternatively spliced Kdap mRNA in keratinocytes, we used the same conditions as before, except for a different annealing temperature (58°C) and a primer set: 5′-CTGCCGTGGTGCTCCTCTCC-3′ and 5′-AGTTGCGCTCCTCAGTCCTTTCA-3′.

Construction of plasmid and adenoviral expression vectors A plasmid expression vector, pKdap-Fc, encoding a fusion protein of human Kdap precursor and an Fc portion of human IgG1, was constructed. Briefly, the entire coding sequence for Kdap precursor was PCR amplified with 5′- and 3′-primers containing *Eco*RI and *Xba*I restriction enzyme sites, respectively. The resulting PCR fragment was inserted in frame into the 5′-end of a coding sequence for the Fc portion that had been subcloned previously into a CMV-driven expression vector (pcDNA3.1, Invitrogen).

Adenoviral vectors (Adv) were generated according to the manufacturer's manuals of AdEasy system (Quantum Biotechnologies, Carlsbad, California) with minor modifications (He *et al*, 1998). A full-length cDNA for the human Kdap precursor was introduced into a CMV-driven shuttle vector (pShuttle-CMV) using *Xho*I and *Eco*RV restriction sites. After linearization of the shuttle vector DNA with *Pme*I, DNA (0.5 μg) was co-transformed into BJ5183 *Escherichia coli* (Quantum Biotechnologies) with 0.1 μg of pAdEasy-1, which encodes a whole genome of Adv type 5 lacking the E1 and E3 regions. The obtained plasmid clones were screened for recombinant Adv DNA by total size (>33 kb) and by presence of the Kdap gene. A plasmid sequence in a selected recombinant DNA (5 μg) was removed by digestion with *Pac*I and then transfected into a permissive cell line, 293A, using 6 μg of FuGENE 6. After culturing for 6 d, recombinant viral particles were recovered by freeze–thawing transfected cells, amplified further by infection of large numbers of 293A cells, and then purified by double ultracentrifugation through cesium chloride gradients. Plaque-forming units (PFU) of purified Adv were determined using the tissue culture infectious dose ($TCID_{50}$) method described previously (He *et al*, 1998).

Gene delivery In plasmid transfection, COS-1 cells were seeded at 1 d prior to transfection onto a 60 mm culture dish at a density of 5×10^5 cells. Cells were incubated overnight in the presence of the expression vector DNA (2 μg) and 6 μL of FuGENE 6. For Adv-mediated gene delivery to COS-1 cells and keratinocytes, cells were seeded on 24-well plates at a density of 1×10^5 cells per well. The next day, recombinant Adv was added at multiplication of infection (MOI) of 250 for COS-1 cells and 500 for keratinocytes. After incubating at 37°C for 90 min, uninfected Adv was washed out and then cultured for 2 d.

Extraction of proteins and SDS-PAGE/western blotting Two days after transfection or infection, the culture medium was replaced with fresh medium. The next day, the supernatant was recovered and whole-cell extracts were prepared by incubating cells with 0.3% Triton X-100/phosphate-buffered saline (PBS) containing 1 mM phenylmethylsulfonyl fluoride (PMSF) and 2 μg per mL of leupeptin, followed by centrifugation (Shikano *et al*, 2001). Whole-cell extracts were also prepared from the scales of psoriatic skin and of dry skin in a healthy individual as described previously (Zeeuwen *et al*, 1997). In experiments assaying Kdap protein expression from the supernatant of cultured keratinocytes (not transfected), the supernatant was concentrated in volume 10–20-fold by lyophilization and subsequently rehydrated with a small volume of buffer.

Aliquots of each fraction prepared from transfected cells or protein extracts from psoriatic scales were size fractionated on 16.5% Tris-Tricine gels under reduced conditions. Following electro-transfer onto Hybond-P membrane (Amersham Pharmacia Biotech, Piscataway, New Jersey), the membranes were blocked with 5% non-fat dried milk/0.1% Tween 20/PBS and incubated with 0.1 μg per mL of purified rabbit IgG raised against His-tagged Kdap recombinant proteins or control IgG. Signals were developed with horseradish peroxidase (HRP)-conjugated goat anti-rabbit IgG and ECL plus system (Amersham Pharmacia Biotech).

Production of antibodies against His-tagged recombinant Kdap protein A bacterial expression vector, pET-hKdap, was constructed by insertion of a PCR-amplified coding sequence for human mature Kdap in frame into that for N-terminal 10 × Histidine in an expression vector, pET-16b (Novagen, Madison, Wisconsin). BL21(DE3) *E. coli* (Novagen) transformed with pET-hKdap was treated with 1 mM IPTG for 6 h. After harvesting cells, whole proteins were extracted by 8 M urea/100 mM sodium acetate/Tris-HCl, pH 8.0, and applied to affinity purification with nickel resins (Quiagen). His-tagged Kdap was eluted from the resins with 8 M urea/100 mM sodium acetate/0.5 M imidazole, pH 4.5, fractions were collected containing proteins, and finally refolded by dialysis against 100 mM phosphate buffer (pH 7.7).

Refolded His-Kdap was used for immunization of rabbits. A mixture of Kdap recombinant proteins (200 μg per rabbit) and complete Freund's adjuvant was injected into rabbits, followed by three boosts with incomplete Freund's adjuvant at 3-wk intervals. Five days after the last boost, serum was collected from immunized rabbits and affinity purified with beads conjugated with His-Kdap.

N-terminal sequencing To determine the exact site of signal peptide cleavage in the Kdap precursor, purified recombinant Kdap-Fc was subjected to N-terminal sequencing. Briefly, 3 d after transfection of pKdap-Fc into COS-1 cells, Fc-fusion proteins in the culture supernatant were allowed to bind to Protein A–agarose (Sigma, St Louis, Missouri), and then eluted sequentially with 150 mM NaCl/50 mM acetate buffer (pH 4.3) and 150 mM NaCl/50 mM glycine buffer (pH 2.3). Fractions with highest protein concentrations were selected and applied to SDS-PAGE, followed by western blotting. A band with reactivity to goat anti-human IgG Ab was purified by gel extraction and subjected to 15 cycles of N-terminal sequencing by automated Edman degradation in the HHMI Protein Chemistry Core Research Facility (UT Southwestern).

Skin samples Biopsies were taken from lesional skin sites of three individuals with psoriasis. Our study was performed after the ethics committee approval and informed consent was obtained under the Declaration of Helsinki Principles. The controls included two normal individuals (one female and one male) without skin disease for fluorescence and for *in situ* hybridization and two different individuals for immunoelectron microscopy (two males).

Indirect Immunofluorescence Human skin cryostat sections were fixed in cold acetone (−20°C) for 10 min and incubated with 5% normal goat serum (NGS) in 0.1 M Dulbecco's PBS for 5 min at 37°C. Sections were incubated with anti-Kdap Ab or rabbit control IgG (diluted at 1:50), secondary antibody goat anti-rabbit IgG fluorescein isothiocyanate (FITC, Dako, Kyoto, Japan), diluted in 3% bovine serum albumin (BSA) in 0.1 M PBS for 30 min at 37°C. The sections were then mounted in Permafluor (Thermo Shandon,

Pittsburgh, Pennsylvania) and examined with a Nikon Optiphot 2 microscope equipped for epifluorescence or a confocal laser inverted microscope (Olympus Fluoview FV300 Optical Elements Corporation, Dulles, VA). Images were scanned sequentially using a 40 times objective, and multiple images were Kalman averaged ($n > 5$).

Post-embedding immunogold electron microscopy Skin samples were obtained from the outer aspect of the arm and thigh, and were processed for post-embedding immunoelectron microscopy as previously described (Shimizu *et al*, 1989). Briefly, samples were cryoprotected in 20% glycerol/PBS for 1 h at 4°C, and plunged in liquid propane at −190°C using a KF-80 apparatus (Reichert Jung, Vienna, Austria). After freeze substitution over 3 d at −80°C in methanol and over 2 d at −60°C using the AFS apparatus (Leica, Milton Keynes, UK), the samples were embedded in Lowicryl K11M resin polymerized by UV light. Ultrathin sections were cut and collected on pioloform-coated nickel grids. The sections were pre-incubated in PBS containing 5% NGS, 1% BSA, and 0.1% gelatin and then incubated with anti-Kdap Ab (1:100 dilution) at 37°C for 2 h. After washing with PBS, the sections were incubated with secondary linker Ab for 2 h at 37°C, followed by incubation with a gold-conjugated antibody for 2 h at 37°C. After staining with alcoholic uranyl acetate (15 min) and Reynolds lead citrate (5 s), the sections were observed in a Hitachi H7100-transmission electron microscope (Hitachi, Tokyo, Japan).

***In situ* hybridization of human skin** This assay was performed using manufacturer's recommendations of mRNA *locator* (Ambion, Austin, Texas). Briefly, frozen skin sections were treated with proteinase K at room temperature for 20 min. After fixation, genomic nucleotides were digested with 500 U per mL DNase I at 37°C for 1 h. Control sections were treated with RNase (instead of DNase). For probe preparation, a full-length cDNA of *Kdap* (441 bp) was subcloned into a pGEM-7zf(−) (Promega, Madison, Wisconsin) and used as a template for *in vitro* RNA synthesis using MAXIscript (Ambion). Anti-sense and sense (negative control) RNA probes were synthesized by T7 and SP6, respectively, RNA polymerase in the presence of biotin-labeled UTP (Invitrogen). DNase-treated sections were then hybridized at 42°C for 24 h with 10 ng per mL biotin-labeled RNA probe. After washing, unhybridized Ribo probes were digested with 1 μg per mL RNase A for 30 min at 37°C, and hybridized probes were then visualized by histochemistry using HRP-labeled streptavidin, avidin-peroxidase, and AEC reagent.

We are grateful to Dr Tasuku Honjo for providing pcDL-SRα-Tac(3′) expression vector, Irene Dougherty and Hideki Nakamura for technical support, and Susan Milberger for administrative assistance. This research was supported partially by Pilot & Feasible Study Skin Disease Research Core (P30 AR41940-10).

DOI: 10.1111/j.0022-202X.2004.22511.x

Manuscript received August 25, 2003; revised November 18, 2003; accepted for publication December 10, 2003

Address correspondence to: Kiyoshi Ariizumi, Department of Dermatology, UT Southwestern Med. Ctr., 5323 Harry Hines Blvd, Dallas, Texas 75390-9069, USA. Email: kiyoshi.ariizumi@utsouthwestern.edu

References

Ariizumi K, Bergstresser PR, Takashima A: Subtractive cDNA cloning. A new approach to understanding dendritic cell biology In: Dendritic Cells in fundamental and Clinical Immunology, (ed.) Ricciardi-Castagnoli. Plenum Press, New York, 1997; p 449–454

Ariizumi K, Meng Y, Bergstresser PR, Takashima A: IFN-γ-dependent IL-7 gene regulation in keratinocytes. J Immunol 154:6031–6039, 1995

Ariizumi K, Shen G-L, Ritter III R, *et al*: Identification of a novel, dendritic cell-associated molecule, Dectin-1, by subtractive cDNA cloning. J Biol Chem 275:20157–20167, 2000

Bonkobara M, Das A, Takao J, Cruz PDJ, Arilzumi K: Identification of genes for secreted and membrane-anchored proteins in keratinocytes. Br J Dermatol 148:654–664, 2003

Chatterjee S, Mayor S: The GPI-anchor and protein sorting. CMLS Cell Mol Life Sci 58:1969–1987, 2001

Cui CY, Aragane Y, Maeda A, Piao YL, Takahashi M, Kim LH, Tezuka T: Bikunin, a serine protease inhibitor, is present on the cell boundary of epidermis. J Invest Dermatol 113:182–188, 1999

de Viragh PA, Huber M, Hohl D: Involucrin mRNA is more abundant in human hair follicles than normal epidermis. J Invest Dermatol 103:815–819, 1994

Girolomoni G, Stone DK, Bergstresser PR, Crutz PDJ: Increased number and microtubule-associated dispersal of acidic intracellular compartments accompany differentiation of cultured human keratinocytes. J Invest Dermatol 98:911–917, 2000

He TC, Zhou S, Da Costa LT, Yu J, Kinzler KW, Vogelstein B: A simplified system for generating recombinant adenoviruses. Proc Natl Acad Sci USA 95:2509–2514, 1998

Ishida-yamamoto A, Iizuka H: Structural organization of cornified cell envelops and alterations in inherited skin disorders. Exp Dermatol 7:1–10, 1998

Jin F, Nathan C, Radzioch D, Ding A: Secretory leukocyte protease inhibitor: A macrophage product induced by and antagonistic to bacterial lipopolysaccharide. Cell 88:417–426, 1997

Kalinin A, Marekov LN, Steinert PM: Assembly of the epidermal cornified cell envelope. J Cell Sci 114:3069–3070, 2001

Lavker RM, Risse B, Brown H, Ginsburg D, Pearson J, Baker MS, Jensen PJ: Localization of plasminogen activator inhibitor type 2 (PAI-2) in hair and nail: Implications for terminal differentiation. J Invest Dermatol 110: 917–922, 1998

Mägert HJ, Kreutzmann P, Ständker L, Walden M, Drögemüller K, Forssmann WG: LEKTI: A multidomain serine proteinase inhibitor with pathophysiological relevance. Int J Biochem Cell Biol 34:573–576, 2001

Molhuizen HO, Schalkwijk J: Structural, biochemical, and cell biological aspects of the serine proteinase inhibitor SKALP/elafin/ESI. Biol Chem Hoppe Seyler 376:1–7, 1995

Nakane H, Ishida-yamamoto A, Takahashi H, Iizuka H: Elafin, a secretory protein, is cross-linked into the cornified cell envelopes from the inside of psoriatic keratinocytes. J Invest Dermatol 119:50–55, 2002

Oomizu S, Sahuc F, Asahina K, *et al*: Kdap, a novel gene associated with the stratification of the epithelium. Gene 256:19–27, 2000

Pfundt R, van Ruissen F, Vlijmen-Willems IMJJV, *et al*: Constitutive and inducible expression of SKALP/elafin provides anti-elastase defense in human epithelia. J Clin Invest 98:1389–1399, 1996

Schalkwijk J, Chang A, Janssen P, De Jongh GJ, Mier PD: Skin-derived anti-leucoproteases (SKALPs): Characterization of two new elastase inhibitors from psoriatic epidermis. Br J Dermatol 122:631–641, 1990

Schalkwijk J, Wiedow O, Hirose S: The trappin gene family: Proteins defined by an N-terminal transglutaminase substrate domain and a C-terminal four-disulphide core. Biochem J 340:569–577, 1999

Shikano S, Bonkobara M, Zukas PK, Ariizumi K: Molecular cloning of a dendritic cell-associated transmembrane protein, DC-HIL, that promotes RGD-dependent adhesion of endothelial cells through recognition of heparan sulfate proteoglycans. J Biol Chem 276:8125–8134, 2001

Shimizu H, McDonald JN, Kennedy AR, Eady RAJ: Demonstration of intra- and extra-cellular localization of bullous pemphigoid antigen using cryofixation and freeze substitution for postembedding immuno-electron microscopy. Arch Dermatol Res 281:443–448, 1989

Sotiropoulou G, Anisowicz A, Sager R: Identification, cloning, and characterization of cystatin M, a novel cysteine, proteinase inhibitor, down-regulated in breast cancer. J Biol Chem 272:903–910, 1997

Steinert PM, Marekov LN: The proteins elafin, filaggrin, keratin intermediate filaments, loricrin, and small proline-rich proteins 1 and 2 are isodipeptide cross-linked components of the human epidermal cornified cell envelope. J Biol Chem 270:17702–17711, 1995

Takahashi M, Tezuka T, Katunuma N: Phosphorylated cystatin a is a natural substrate of epidermal transglutaminase for formation of skin cornified envelope. FEBS Lett 308:79–82, 1992

Tashiro K, Nakano T, Honjo T: Signal sequence trap, expression cloning method for secreted proteins and type 1 membrane proteins. Methods Mol Biol 69:203–219, 1997

Tashiro K, Tada H, Heilker R, Shirozu M, Nakano T, Honjo T: Signal sequence trap: A cloning strategy for secreted proteins and type I membrane proteins. Science 261:600–602, 1993

Watt FM: Terminal differentiation of epidermal keratinocytes. Curr Opin Cell Biol 1:1107–1115, 2000

Wiedow O, Schroder JM, Gregory H, Young JA, Christophers E: Elafin: An elastase-specific inhibitor of human skin. Purification, characterization, and complete amino acid sequence. J Biol Chem 265:14791–14795, 1990

Wilson IB, Gavel Y, von Heijne G: Amino acid distributions around O-linked glycosylation sites. Biochem J 275:529–534, 1991

Zeeuwen PLJM, Henriks W, de Jong WW, Schalkwijk J: Identification and sequence analysis of two new members of the SKALP/elafin and SPAI-2 gene family. J Biol Chem 272:20471–20478, 1997

Zeeuwen PLJM, Vlijmen-Willems IMJJV, Jansen BJH, *et al*: Cystatin M/E expression is restricted to differentiated epidermal keratinocytes and sweat glands: A new akin-specific proteinase inhibitor that is a target for cross-linking by transglutaminase. J Invest Dermatol 116:693–701, 2001

THE JOURNAL OF BIOLOGICAL CHEMISTRY
Vol. 279, No. 3, Issue of January 16, pp. 1676–1683, 2004
Printed in U.S.A.

Ultraviolet A-induced Production of Matrix Metalloproteinase-1 Is Mediated by Macrophage Migration Inhibitory Factor (MIF) in Human Dermal Fibroblasts*

Received for publication, April 8, 2003, and in revised form, October 10, 2003
Published, JBC Papers in Press, October 27, 2003, DOI 10.1074/jbc.M303650200

Hirokazu Watanabe‡, Tadamichi Shimizu‡, Jun Nishihira§, Riichiro Abe‡, Toshinori Nakayama¶‖, Masaru Taniguchi‖, Hisataka Sabe‡‡, Teruo Ishibashi§, and Hiroshi Shimizu‡§§**

*From the Departments of ‡Dermatology and §Molecular Biochemistry, Hokkaido University Graduate School of Medicine, Kita-ku, Sapporo 060-8638, Japan, the ¶Department of Medical Immunology and ‖Department of Molecular Immunology, Graduate School of Medicine, Chiba University, 1-8-1 Inohana Chuo-ku, Chiba 260-8670, Japan, the **Laboratory for Immune Regulation, RIKEN Research Center for Allergy and Immunology, Yokohama, 230-0045, Japan, and the ‡‡Department of Molecular Biology, Osaka Bioscience Institute, Osaka 565-0874, Japan*

Matrix metalloproteinases (MMPs) are thought to be responsible for dermal photoaging in human skin. In the present study, we evaluated the involvement of macrophage migration inhibitory factor (MIF) in MMP-1 expression under ultraviolet A (UVA) irradiation in cultured human dermal fibroblasts. UVA (20 J/cm^2) up-regulates MIF production, and UVA-induced MMP-1 mRNA production is inhibited by an anti-MIF antibody. MIF (100 ng/ml) was shown to induce MMP-1 in cultured human dermal fibroblasts. We found that MIF (100 ng/ml) enhanced MMP-1 activity in cultured fibroblasts assessed by zymography. Moreover, we observed that fibroblasts obtained from MIF-deficient mice were much less sensitive to UVA regarding MMP-13 expression than those from wild-type BALB/c mice. Furthermore, after UVA irradiation (10 J/cm^2), dermal fibroblasts of MIF-deficient mice produced significantly decreased levels of MMP-13 compared with fibroblasts of wild-type mice. Next we investigated the signal transduction pathway of MIF. The up-regulation of MMP-1 mRNA by MIF stimulation was found to be inhibited by a PKC inhibitor (GF109203X), a Src-family tyrosine kinase inhibitor (herbimycin A), a tyrosine kinase inhibitor (genistein), a PKA inhibitor (H89), a MEK inhibitor (PD98089), and a JNK inhibitor (SP600125). In contrast, the p38 inhibitor (SB203580) was found to have little effect on expression of MMP-1 mRNA. We found that PKC-pan, PKCα/βII, PKCδ (Thr505), PKCδ (Ser^{643}), Raf, and MAPK were phosphorylated by MIF. Moreover, we demonstrated that phosphorylation of PKCα/βII and MAPK in response to MIF was suppressed by genistein, and herbimycin A as well as by transfection of the plasmid of C-terminal Src kinase. The DNA binding activity of AP-1 was significantly up-regulated 2 h after MIF stimulation. Taken together, these results suggest that MIF is involved in the up-regulation of UVA-induced MMP-1 in dermal fibroblasts through PKC-, PKA-, Src family tyrosine kinase-, MAPK-, c-Jun-, and AP-1-dependent pathways.

The skin is an important barrier that protects the body from damage due to direct contact with the outside environment, including trauma, bacterial infection, and ultraviolet (UV) irradiation. Regarding the environmental damage to skin, the most common physical injury is that caused by UV irradiation. UV irradiation substantially increases the risk of actinic damage to the skin. Interstitial collagens, the major structural components of the dermis, have been found to be particularly diminished in skin actinically damaged by UV irradiation (1–3). Quantitative and qualitative changes in the dermal extracellular matrix proteins such as elastin, glycosaminoglycans, and interstitial collagens are also associated in dermal photodamage. There are several morphological and biochemical indications that collagen type I is reduced in UV actinically damaged skin (4). Various types of UV-induced matrix-degenerating metalloproteinases present in dermal fibroblasts contribute to the breakdown of dermal interstitial collagen and other connective tissue components.

As for the underlying biological mechanisms of action involved in skin damage, the skin is known to secrete a number of cytokines, including interleukin (IL)[1]-1, IL-6, and tumor necrosis factor (TNF)-α (5–7). UV irradiation up-regulates the production of these cytokines, and UV-induced collagenases such as matrix metalloproteinase (MMP)-1 from dermal fibroblasts are mediated in part by IL-1α and IL-1β (6). Furthermore, collagenase activity has been shown to be inhibited by a tissue inhibitor of metalloproteinases (TIMP) (8).

Macrophage migration inhibitory factor (MIF), originally identified as a lymphokine that concentrates macrophages at inflammatory loci, is a potent activator of macrophages *in vivo* and is considered to play an important role in cell-mediated immunity (9, 10). It has been reported that MIF is expressed primarily by T cells and macrophages; recent studies have however revealed that this protein is ubiquitously expressed by various cells, thus indicating its involvement beyond the immune system in a variety of pathologic states (11, 12). It is of interest that MIF functions as a cytokine, an anterior pitu-

* This work was supported in part by Grants-in-aid for research (No. 11670813 and 13357008) from the Ministry of Education, Science, and Culture of Japan, and the Shiseido Foundation for Skin Aging Research. The costs of publication of this article were defrayed in part by the payment of page charges. This article must therefore be hereby marked "*advertisement*" in accordance with 18 U.S.C. Section 1734 solely to indicate this fact.

§§ To whom correspondence should be addressed: Dept. of Dermatology, Hokkaido University Graduate School of Medicine, Sapporo 060-8638, Japan. Fax: 81-11-706-7820; E-mail: shimizu@med.hokudai.ac.jp.

[1] The abbreviations used are: IL, interleukin; MIF, macrophage migration inhibitory factor; MMP, matrix metalloproteinase; UV, ultraviolet; TNF-α, tumor necrosis factor-α; TIMP, tissue inhibitor of matrix metalloproteinase; JNK, c-Jun N-terminal kinase; EMSA, electrophoretic gel mobility shift assay; CSK, C-terminal Src kinase; PKC, protein kinase C; FCS, fetal calf serum; DMEM, Dulbecco's modified Eagle's medium; WT, wild type; ELISA, enzyme-linked immunosorbent assay; MAPK, mitogen-activated protein kinase; DAG, diacylglycerol-PKA, cAMP-dependent protein kinase.

itary-derived hormone, and a glucocorticoid-induced immunomodulator (13).

It is of note that UVA irradiation reaches the reticular dermis, rendering fibroblasts accessible targets (14). In the skin, MIF is expressed in the epidermis, particularly in the basal layer (15). However, the precise role of MIF in the dermis and the effects of UVA on MIF expression of dermal fibroblasts remain unknown. In the present study, we attempted to determine whether MIF mediates the up-regulation of MMP-1 expression in response to the stimulation of UVA irradiation. We also investigated the signal transduction pathway of MIF in human dermal fibroblasts.

EXPERIMENTAL PROCEDURES

Materials—The following materials were obtained from commercial sources. Genistein, herbimycin A, PP2, GF109203X, H89, PD98089, SB203580, and SP600125 were purchased from Calbiochem (San Diego, CA); Dulbecco's modified Eagle's medium (DMEM) from Invitrogen (Groningen, Netherland); Dig Gel Shift kit and FuGENE 6 was from Roche Applied Science (Mannheim, Germany); the Isogen RNA extraction kit was from Nippon Gene (Toyama, Japan); the Biotrack MMP-1 assay kit, [α-^{32}P]dCTP, and Hybond N nylon membrane were from Amersham Biosciences (Piscataway, NJ); the consensus AP-1 oligonucleotide was from Promega (Madison, WI); the DNA random primer labeling kit was from Takara (Kyoto, Japan); anti-phospho-PKCpan, PKCα/βII (Thr$^{638/641}$), PKCδ (Thr^{505}), PKCδ (Ser^{643}), PKCθ (Thr^{538}), PKD/PKCμ (Ser$^{744/748}$), PKD/PKCμ (Ser^{916}), PKCζ/λ (Thr$^{410/403}$); anti-phospho-Raf, anti-phospho-p44/p42 MAPK antibodies, and the phototope-HRP Western blot detection system were from Cell Signaling Technology (Beverly, MA); Anti-MMP-1, anti-β-actin antibodies and gelatin were purchased from Sigma-Aldrich Co.; anti-MMP-13 (Collagenase-3) antibody was from Chemicon (Temecula, CA); YM-30 was from Millipore (Bedford, MA); and recombinant human MMP-1 was from Genzyme-Techne (Minneapolis, MN). The anti-MIF polyclonal antibody was prepared as described previously (15). Recombinant human MIF was expressed in *Escherichia coli* BL21/DE3 (Novagen, Madison, WI) and purified as described previously (16). This MIF contained less than 1 pg of endotoxin per μg of protein, as determined by chromogenic Lumulus amoebocyte assay (BioWhittaker, Walkerville, MD). Plasmids of C-terminal Src kinase (CSK) and dominant negative mutant of CSK (CSK$^-$) were prepared as previously described (17).

Cells and Skin Tissues—Human dermal fibroblasts were purchased from Dainippon Seiyaku (Osaka, Japan). Cells of passages 3–4 were used for the experiments. In brief, cells were maintained in DMEM supplemented with 10% heat-inactivated FCS, glutamine (2 mM), sodium ascorbate (50 μg/ml), penicillin (100 units/ml), streptomycin (100 μg/ml), and fungizone (100 μg/ml). The cells were grown in a moist atmosphere in a 5% CO_2 incubator at 37 °C.

MIF-deficient mice were established by targeted disruption of the MIF gene, using a mouse strain bred onto a BALB/c background (18). Wild-type (WT) BALB/c mice were purchased from Japan Clea (Shizuoka, Japan) and maintained under specific-pathogen-free conditions. Mouse dermal fibroblasts were obtained from MIF-deficient mice and control WT mice. Newborn mouse skin was carefully shaven, a segment of skin excised, and fibroblasts were obtained using the standard explant technique. Briefly, the skin was cut into 3 × 5-mm pieces and placed onto large Petri dishes with the subcutaneous side down. Once a sufficient number of fibroblasts had migrated out from the skin sections, pieces of the skin were removed and the cells were passaged by trypsin digestion in the same manner as for the fibroblasts. Fibroblasts were grown in DMEM containing 10% FCS and penicillin/streptomycin. The cells from passage 3 were used for the experiment.

UVA Irradiation—Human dermal fibroblasts were washed twice with phosphate-buffered saline. The UVA irradiation source was a FL20S/BLB fluorescent lamp (Clinical Supply, Tokyo, Japan) that emitted an energy spectrum with high fluency in the UVA region (300–430 nm), with a peak at 352 nm. A 6-mm thick glass plate was used to block UVB emissions. The emitted dose was calculated using a UVA radiometer photodetector (Torex, Tokyo, Japan). The cells were washed with phosphate-buffered saline, suspended in Hank's buffer, and subjected to UVA irradiation. The duration of UV irradiation delivered to cells was altered by sliding a plastic lid covered with aluminum foil onto a flat-bottomed 6-well plate. After irradiation, the cells were cultured in DMEM with 10% FCS at 37 °C. Control samples were mock-irradiated and maintained under the same culture conditions as those used for the UVA-irradiated specimens. To examine the effects of anti-MIF antibody on the UVA-induced MMP-1 mRNA, fibroblasts were UVA-irradiated (20 J/cm^2) in the presence of an anti-MIF antibody (1 and 10 μg/ml) in DMEM supplemented with 10% FCS and then further incubated for 24 h. Expression of MMP-1 mRNA and protein levels were assessed by Northern blot and Western blot analyses. The abdomens of MIF-deficient mice or WT mice were carefully shaved, and irradiated with UVA (0–30 J/cm^2). After UVA irradiation for 24 h, skin was surgically obtained and MMP-13 production was assessed by Western blot analysis. Dermal fibroblasts from MIF-deficient mice or WT mice were harvested after reaching 70% confluence. The cells were washed twice with PBS and exposed to a UVA fluorescent lamp for the indicated doses (0–10 J/cm^2). After irradiation, cells were cultured in DMEM supplemented with 10% FCS for 24 h, and MMP-13 production was evaluated by Western blot analysis.

Northern Blot Analysis—Complete coding cDNA for human MMP-1 in a pSP64 vector was obtained from the American Type Culture Collection. Templates of human TIMP-1 and glyceraldehyde-3-phosphate dehydrogenase (GAPDH) cDNA for Northern blot analyses were obtained by reverse transcription-polymerase chain reaction (RT-PCR) from a human cDNA library of human primary dermal fibroblasts. Preparation of each template proceeded using the following primers: TIMP-1 (535 bp), forward primer 5′-TCCTGTTGTTGCTGTGGCTGATAGC-3′ and reverse primer 5′-CAGGCAAGGTGACGGGACTGGAAGC-3′, GAPDH (306 bp), forward primer 5′-CGGAGTCAACGGATTTGGTCGTAT-3′ and reverse primer 5′-AGCCTTCTCCATGGTGGTGAAGAC-3′. To examine the signal transduction pathway of MIF, human dermal fibroblasts were stimulated with or without MIF and various inhibitors of molecules involved in the signal transduction pathway for 24 h. Total RNA was isolated from monolayered cultures using an Isogen RNA extraction kit according to the manufacturer's protocols. RNA was quantified by spectrophotometry, and equal amounts of RNA (5–10 μg) from samples were loaded on a formaldehyde-agarose gel. The gel was stained with ethidium bromide to visualize the RNA standards, and the RNA was transferred onto a nylon membrane. Fragments obtained by restriction enzyme treatments for MMP-1, TIMP-1, GAPDH, and MIF were labeled with [α-^{32}P]dCTP using a DNA random primer labeling kit. Hybridization was carried out at 42 °C for 24 h. Post-hybridization washes were performed twice in 0.1% SDS, 0.2× SSC (1× SSC: 0.15 M NaCl, 0.015 M sodium citrate) at 65 °C for 15 min. The radioactive bands were visualized by autoradiography on Kodak X-AR5 film and quantitatively analyzed using the NIH Image system. Multiple autoradiographic data were examined to ensure that the results reflected those produced in the linear range of the film. The results were normalized by GAPDH mRNA levels. Comparison of ethidium bromide-stained gels with the corresponding GAPDH mRNA levels showed that GAPDH mRNA levels reflected the total RNA loaded onto the gels.

ELISA for MIF—To examine the concentration of MIF from cultured fibroblasts, supernatants from cultured fibroblasts by UVA were examined using an MIF ELISA system essentially as described previously (19). For this assay we used recombinant human MIF to obtain the standard curve, in which good linearity was demonstrated between MIF concentrations (1 to 200 ng/ml) and absorbency.

ELISA for MMP-1—After reaching confluence, the cells were trypsinized and then plated on a 24-well culture dish at 4 × 10^4 cells per well in 0.5 ml of DMEM containing 10% FCS. After 48 h, the medium was replaced with 0.5 ml of serum-free DMEM containing various doses of MIF (0, 0.1, 1, 10, and 100 ng/ml). After 24 h, the supernatants were collected and subjected to ELISA for MMP-1. The protein level values for MMP-1 were added to those of the supernatants. For the time-course study, we used a procedure similar to that used for the dose response study in the presence of 100 ng/ml MIF using human dermal fibroblasts. Aliquots were obtained at the indicated intervals for up to 48 h. MMP-1 was assayed by an ELISA using a Biotrack MMP-1 assay kit according to the manufacturer's protocol. The minimal sensitivity of the assay system was 6.25 ng/ml, and good linearity was observed at amounts up to 100 ng/ml. Using this ELISA system, all forms of MMP, including pro-MMP-1, MMP-1, and MMP-1 complexes with TIMP-1, could be measured.

Determination of MMP-1 Activity in Culture Media of Fibroblasts—Culture media of dermal fibroblasts were collected at the indicated intervals in the presence of MIF (100 ng/ml) for up to 48 h, and concentrated (10-fold) using Centriprep YM-30 (Millipore, Bedford, MA) for further analyses. Then, MMP-1 activities were determined by heparin-enhanced zymography as previously described (20). In brief, gelatin (0.5 mg/ml) was embedded in 7.5% SDS-PAGE gel. Samples (15 μg protein for each sample) were treated with sample buffer without dithiothreitol at room temperature and electrophoresed until the dye-

front was near the bottom of the gel. To produce the enhancing effects, 10 ml heparin (0.3 mg/ml in 1× sample buffer without SDS) was added to the lanes 20–30 min after electrophoresis began. Each gel was washed two times with 2.5% Triton X-100, 50 mM Tris, pH 7.5, 4 °C, 20 min each, to remove SDS and then two times with buffer plus 5 mM $CaCl_2$. The gel was washed three times with incubation buffer (50 mM Tris, pH 7.5, 5 mM $CaCl_2$) and then incubated in this buffer with added protease inhibitors (50 μM each of z-phe-chloromethylketone and tosyl-phe-chloromethylketone and aminoethyl benzenesulfonyl fluoride) for 18 h at 37 °C with gentle shaking. Gels were stained with 0.1% Coomassie Blue in 40% MeOH, 10% acetic acid, for 45 min, and destained with 7% acetic acid. A positive control for recombinant human MMP-1 was used to detect the molecules of MMP-1.

Western Blot Analysis—Cells (1×10^6 cells) were disrupted with a Polytron homogenizer (Kinematica, Lucerne, Switzerland). The protein concentrations of the cell homogenates were quantified using a Micro BCA protein assay reagent kit. Equal amounts of homogenates were dissolved in 20 μl of Tris-HCl, 50 mM (pH 6.8), containing 2-mercaptoethanol (1%), sodium dodecyl sulfate (SDS) (2%), glycerol (20%), and bromphenol blue (0.04%), and the samples were heated to 100 °C for 5 min. The samples were then subjected to SDS-PAGE and transferred electrophoretically onto a nitrocellulose membrane. The membranes were blocked with 1% nonfat dry milk in phosphate-buffered saline, probed with anti-phospho-Raf, or anti-phospho-MAPK antibody, then allowed to react with goat anti-rabbit IgG Ab coupled with horseradish peroxidase. The resultant complexes were processed for the detection system according to the manufacturer's protocol. To investigate the involvement of tyrosine kinase in PKC phosphorylation, cells were serum-starved for 24 h and challenged with MIF (100 ng/ml) 30 min after the addition of PP2 (10 μM), tyrosine kinase inhibitor (genistein) (100 μM), and Src family tyrosine kinase inhibitor (Herbimycin A) (10 μM) in serum-free medium. After 60 min, the cells were harvested and subjected to Western blot analysis for phosphorylation of phospho-PKCα/βII. To investigate the involvement of tyrosine kinase and PKC in the phosphorylation of MAPK by MIF, fibroblasts pretreated with inhibitors against tyrosine kinase and PKC for 30 min were stimulated by MIF for 60 min. Then cell lysates were prepared and subjected to Western blot analysis. For loading controls, we carried out Western blot analysis on β-actin using an anti-β-actin antibody.

Transfection of CSK and CSK$^-$—At 24 h after plating the fibroblasts on 6-well dishes, plasmid DNAs of CSK and CSK$^-$ were transfected using FuGENE 6 according to the manufacturer's protocol. For each dish, CSK or CSK$^-$ plasmid (1 μg) was transfected to cultured cells in serum-free medium for 24 h. Following this, cells were stimulated with MIF (100 ng/ml) for 60 min. The cell lysates were prepared and subjected to Western blot analysis for phosphorylation of PKC and MAPK.

Electrophoretic Gel Mobility Shift Assay (EMSA)—Human dermal fibroblasts were incubated with 100 ng/ml MIF for the indicated times, and the nuclear proteins extracted. The consensus AP-1 oligonucleotide was annealed and labeled with digoxigenin-11-ddUTP. To prevent nonspecific binding, 0.1 μg of poly(d(I-C)) was added to the binding reaction. The mixture was transferred to a 6% polyacrylamide gel and submitted to gel electrophoresis. Following electrophoresis, the oligonucleotide-protein complexes were electroblotted to a Nylon membrane. The digoxigenin-labeled DNA oligonucleotides were visualized by an enzyme immunoassay using anti-digoxigenin-AP, Fab-fragments, and the chemiluminescent substrate CSPD, as described by the manufacturer (Roche Applied Science). The generated chemiluminescence was visualized on x-ray film.

Statistics—Values are expressed as means ± S.E. of the respective test or control group. Statistical significances between the control group and test groups were evaluated by the Student's *t* test. Data are representative of at least three experiments.

RESULTS

MIF Production in Response to UVA Irradiation in Human Dermal Fibroblasts—We first examined whether UVA is able to stimulate production of MIF in dermal fibroblasts. Fibroblasts were stimulated by UVA, and it was found that UVA up-regulates MIF production in a dose-dependent manner (Fig. 1). After 24-hr UVA stimulation at an intensity of 20 J/cm^2, the MIF content was remarkably elevated, showing a more than 8-fold increase compared with levels in the absence of UVA stimulation.

Effects of MIF on MMP-1 and TIMP-1 mRNA Expression—In human dermal fibroblasts, MMP-1 mRNA was up-regulated in

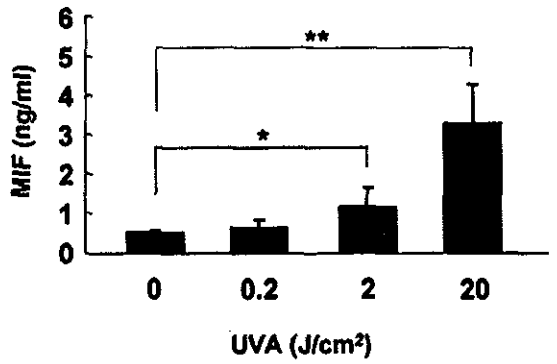

FIG. 1. **Induction of MIF in human fibroblasts by UVA radiation.** *Fibroblasts were treated with UVA radiation and cultured for 24 h. MIF in the culture media was measured by ELISA, as described under "Experimental Procedures." The values are the mean ± S.E. of three different experiments. **, $p < 0.01$ and *, $p < 0.05$ for 20 J/cm^2 versus 0 J/cm^2.*

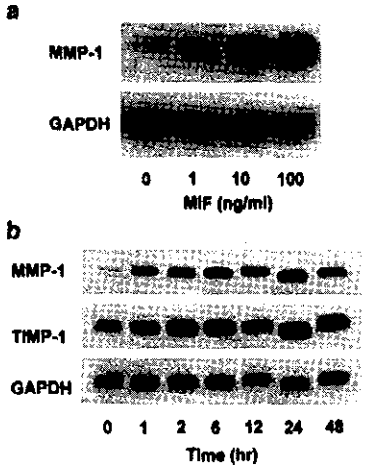

FIG. 2. **Effects of MIF on MMP-1 mRNA expression in dermal fibroblasts.** Total RNAs extracted from dermal fibroblasts were treated with various concentrations of MIF in serum-free medium at the indicated intervals. Northern blot analysis was carried out as described under "Experimental Procedures." The membranes were hybridized with radiolabeled cDNA probes of MMP-1 and GAPDH and then visualized by autoradiography. *a*, the dose-dependent expression of MMP-1 mRNA expression in response to MIF ranging from 0 to 100 ng/ml after 24 h-MIF stimulation. *b*, time-dependent expression of MMP-1 mRNA in response to MIF (100 ng/ml).

a dose-dependent manner in response to MIF, ranging from 1 ng/ml to 100 ng/ml for per 24-hr treatment (Fig. 2*a*). A time-course study of MMP-1 and TIMP-1 in dermal fibroblasts was then performed. MMP-1 mRNA expression increased in response to MIF (100 ng/ml) at 1 h post stimulation and reached a maximum at 24 h (Fig. 2*b*). MIF mRNA levels were slightly down-regulated at 48 h. TIMP-1 mRNA was also elevated, but the increase was less significant than MMP-1 mRNA, although the levels were sustained for at least 48 h.

MMP-1 Production and Activation in Response to MIF—MMP-1 protein was detected in the culture supernatant of human dermal fibroblasts. In a dose-response study, the MMP-1 protein levels were significantly up-regulated at doses of 100 ng/ml (Fig. 3*a*). For the time-course study, MMP-1 in the supernatant was elevated at 12 h after MIF stimulation (100 ng/ml), reached a maximum at 24 h, and was sustained for at least 48 h (Fig. 3*b*). To investigate MIF induced MMP-1 activity, zymography was performed. We used heparin to enhance the signal, because MMP-1 is difficult to detect at low levels in

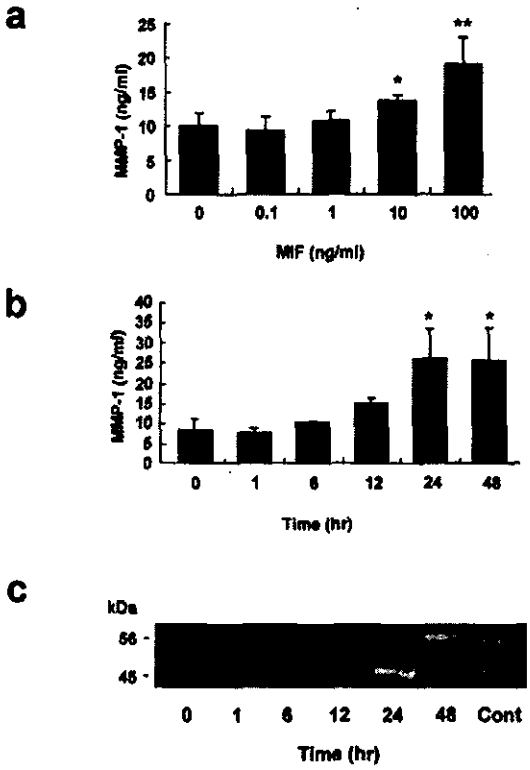

FIG. 3. **Effects of MIF on the production and activation of MMP-1 in dermal fibroblasts.** *a*, aliquots of the culture supernatants of dermal fibroblasts in serum-free medium were collected after treatment with various concentrations of MIF for 24 h, then subjected to ELISA for MMP-1 ($n = 5$). **, $p < 0.01$ and *, $p < 0.05$ *versus* control (0 ng/ml). *b*, culture supernatants of dermal fibroblasts were collected at the indicated times in the presence of 100 ng/ml MIF for up to 48 h and then subjected to ELISA on MMP-1 ($n = 5$), *, $p < 0.05$ *versus* control (0 h). *c*, culture supernatants of dermal fibroblasts were collected at the indicated times in the presence of 100 ng/ml MIF for up to 48 h. The supernatants were concentrated 10-fold and subjected to heparin-enhanced zymography. Molecular weight markers at 56 and 45 kDa show latent and active forms of MMP-1, respectively. *Cont*, stimulation with recombinant MMP-1 for 48 h.

conventional gelatin zymography (20). MMP-1 in the active form (45 kDa) in fibroblasts was enhanced by 100 ng/ml MIF stimulation, reached a maximum at 24 h, and slightly decreased at 48 h (Fig. 3*c*).

Inhibition of MMP-1 Production of Dermal Fibroblasts by a Neutralizing anti-MIF Antibody—We attempted to determine whether neutralizing anti-MIF antibody influences UVA-induced MMP-1 expression in human dermal fibroblasts. By Northern blot analysis, we found that the anti-MIF antibody (1 and 10 μg/ml) significantly down-regulated the expression of MMP-1 mRNA induced by UVA stimulation (20 J/cm^2) (Fig. 4*a*). Based on the results of the Western blot analysis, we confirmed that MMP-1 production is inhibited by the anti-MIF antibody (Fig. 4*b*).

UVA-induced MMP-13 Production in Cultured Dermal Fibroblasts and Skin Tissue in Vivo from MIF-deficient Mice—To clarify whether synthesis of MIF is required for the UVA-induced collagenase, we used dermal fibroblasts from MIF-deficient mice in the production of mouse collagenase MMP-13. Although MMP-13 plays a restricted role in human tissues, it is the predominant tissue collagenase in rodents. Twenty-four hours after UVA irradiation, a significant decrease in viability was observed only after more than 15 J/cm^2 UVA irradiation in fibroblasts from MIF-deficient mouse (data not shown); we therefore used up to 10 J/cm^2 UVA irradiation for experiment.

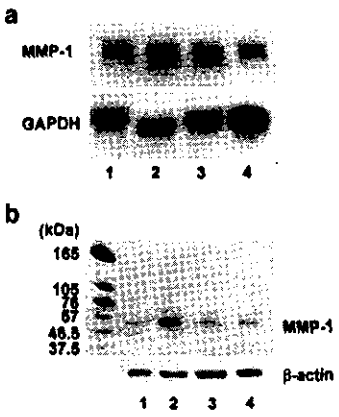

FIG. 4. **Effects of anti-MIF antibody on the UVA-induced MMP-1 mRNA.** *a*, fibroblasts were irradiated (UVA 20 J/cm^2) in the presence of an anti-MIF antibody (1 and 10 μg/ml) in DMEM supplemented with 10% FCS and then further incubated for 24 h. Expression of MMP-1 mRNA was assessed by Northern blot analysis. *Lane 1*, untreated dermal fibroblasts; *lane 2*, fibroblasts stimulated by UVA; *lane 3*, UVA-stimulated fibroblasts with the anti-MIF antibody (1 μg/ml); *lane 4*, UVA-stimulated fibroblasts with the anti-MIF antibody (10 μg/ml). *b*, cell lysates (40 μg) of 20 J/cm^2 UVA-stimulated fibroblasts with anti-MIF antibodies (1 and 10 μg/ml) cultured for 24 h were subjected to Western blot analysis using an anti-MIF antibody. The results with anti-β-actin antibody are shown as a control. *Lane 1*, untreated dermal fibroblasts; *lane 2*, fibroblasts stimulated by UVA; *lane 3*, UVA-stimulated fibroblasts with the anti-MIF antibody (1 μg/ml); *lane 4*, UVA-stimulated fibroblasts with the anti-MIF antibody (10 μg/ml).

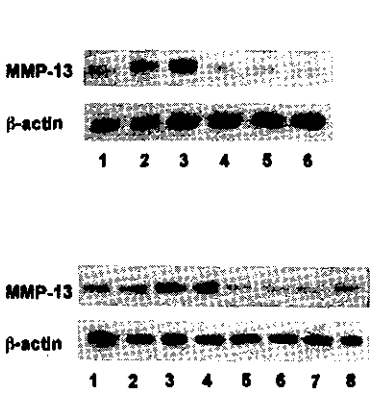

FIG. 5. **UVA-induced MMP-13 production from cultured dermal fibroblasts and skin tissues of MIF-deficient mice.** *a*, cultured 3rd passage dermal fibroblasts from MIF-deficient mice or BALB/c WT mice were irradiated with UVA at 0, 5, 10 J/cm^2. After 24 h, cell lysates (40 μg) were subjected to Western blot using anti-MMP-13 antibody. The results with anti-β-actin antibody are shown as a control. *Lane 1*, WT mouse, 0 J/cm^2; *lane 2*, WT mouse, 5 J/cm^2; *lane 3*, WT mouse, 10 J/cm^2; *lane 4*, MIF-deficient mouse, 0 J/cm^2; *lane 5*, MIF-deficient mouse, 5 J/cm^2; *lane 6*, MIF-deficient mouse 10 J/cm^2. *b*, shaved abdomens of MIF-deficient mice or BALB/c WT mice were irradiated with UVA at 0, 10, 20, and 30 J/cm^2. After 24 h, skin homogenates were subjected to Western blotting using an anti-MMP-13 antibody. *Lane 1*, WT mouse with 0 J/cm^2; *lane 2*, WT mouse with 10 J/cm^2; *lane 3*, WT mouse with 20 J/cm^2; *lane 4*, WT mouse with 30 J/cm^2; *lane 5*, MIF-deficient mouse with 0 J/cm^2; *lane 6*, MIF-deficient mouse with 10 J/cm^2; *lane 7*, MIF-deficient mouse with 20 J/cm^2; *lane 8*, MIF-deficient mouse with 30 J/cm^2.

After 24 h of UVA irradiation (0–10 J/cm^2), elevated MMP-13 production was observed in cell lysates of dermal fibroblasts in control WT mice in a dose-dependent manner (Fig. 5*a*). On the other hand, UVA irradiation appeared to have no effect on MMP-13 production in dermal fibroblasts of MIF-deficient mice. Consistent with these results *in vitro*, elevated MMP-13 production was also observed in the skin of control WT mice in

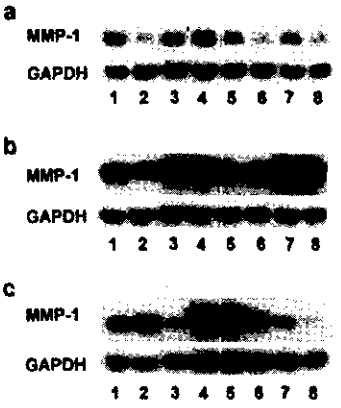

FIG. 6. **Effects of reagents on MIF-induced MMP-1 mRNA expression.** Dermal fibroblasts were preincubated for 30 min with various concentrations of inhibitors prior to challenge with MIF. The cells were then incubated for 24 h in the presence or absence of inhibitors and visualized by autography. *a*, tyrosine kinase inhibitor genistein and Src family tyrosine kinase inhibitor herbimycin A; *lane 1*, no stimulation; *lane 2*, genistein 100 μM; *lane 3*, herbimycin A 10 μM; *lane 4*, MIF 100 ng/ml; *lane 5*, MIF 100 ng/ml + genistein 10 μM; *lane 6*, MIF 100 ng/ml + genistein 100 μM; *lane 7*, MIF 100 ng/ml + herbimycin A 1 μM; *lane 8*, MIF 100 ng/ml + herbimycin A 10 μM. *b*, MEK inhibitor PD98089 and p38 inhibitor SB203580; *lane 1*, no stimulation; *lane 2*, PD98059 40 μM; *lane 3*, SB203580 10 μM; *lane 4*, MIF 100 ng/ml; *lane 5*, MIF 100 ng/ml + PD98059 10 μM; *lane 6*, MIF 100 ng/ml + PD98059 40 μM; *lane 7*, MIF 100 ng/ml + SB203580 5 μM; *lane 8*, MIF 100 ng/ml + SB203580 10 μM. *c*, PKA inhibitor H89 and PKC inhibitor GF109203X. *Lane 1*, no stimulation; *lane 2*, H89 10 μM; *lane 3*, GF109203X 10 μM; *lane 4*, MIF 100 ng/ml; *lane 5*, MIF 100 ng/ml + H89 1 μM; *lane 6*, MIF 100 ng/ml + H89 10 μM; *lane 7*, MIF 100 ng/ml + GF109203X 1 μM; *lane 8*, MIF 100 ng/ml + GF109203X 10 μM.

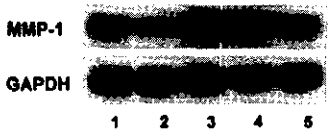

FIG. 7. **Effects of JNK inhibitor on MIF-induced MMP-1 mRNA expression.** Dermal fibroblasts were preincubated for 30 min with various concentrations of inhibitors prior to challenge with MIF similar to the procedure in Fig. 6. The cells were then incubated for 24 h in the presence or absence of JNK inhibitor SP600125. *Lane 1*, no stimulation; *lane 2*, SP600125 30 μM; *lane 3*, MIF 100 ng/ml; *lane 4*, MIF 100 ng/ml + SP600125 3 μM; *lane 5*, MIF 100 ng/ml + SP600125 30 μM.

a dose-dependent manner after UV irradiation *in vivo*, whereas UVA irradiation had little effect on MMP-13 production in the skin of MIF-deficient mice (Fig. 5*b*).

Effects of Inhibitors on MMP-1 Expression in Response to MIF—To examine the signal transduction pathway of MIF, we examined the effects of several inhibitors of molecules involved in the signal transduction pathway when dermal fibroblasts were stimulated with MIF relevant to MMP-1 up-regulation. Several inhibitors were tested, including tyrosine kinase inhibitors genistein and herbimycin A, PKA inhibitor H89, PKC inhibitor GF109203X, and MEK inhibitor PD98089. We found that these inhibitors for tyrosine kinase, PKA, PKC, and MEK inhibitors significantly reduced MMP-1 mRNA stimulated by MIF (Fig. 6, *a–c*). In contrast, the SB203580 (p38 inhibitor) failed to inhibit the up-regulation of MMP-1 mRNA (Fig. 6*b*). Furthermore, we found that JNK inhibitor SP600125 also significantly suppressed MMP-1 mRNA stimulated by MIF (Fig. 7).

Phosphorylation of PKC, Raf, and MAPK—We investigated the phosphorylation of PKC, Raf, and MAPK after MIF stimulation in dermal fibroblasts. The phosphorylation of PKC pan, PKCα/βII, PKCδ (Thr^{505}) and PKCδ (Ser^{643}) reached a maximum level at 30 min in response to MIF, and was down-regulated after 120 min, whereas PKCζ/λ (Thr$^{410/403}$) was not phosphorylated (Fig. 8). Other PKC isoforms, including PKD/PKCμ (Ser$^{744/748}$), PKD/PKCμ (Ser^{916}), and PKCθ (Thr^{538}), were not phosphorylated (data not shown). The phosphorylation of Raf reached a maximum level at 15 min, and that of MAPK was at a maximum level at 60 min (Fig. 9).

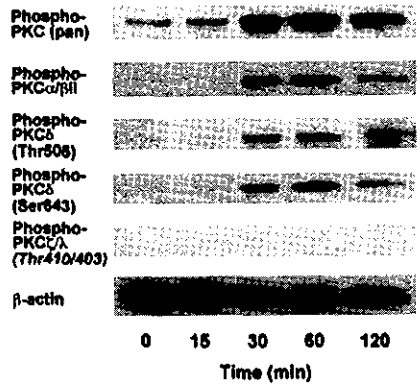

FIG. 8. **Phosphorylation of PKC in response to MIF.** Dermal fibroblasts were stimulated for the indicated time intervals (0–120 min) by MIF (100 ng/ml). Western blot analysis was performed on whole cell lysates (40 μg) and antibodies against phospho-PKCpan, PKCα/βII, PKCδ (Thr^{505}), PKCδ (Ser^{643}), and PKCζ/λ (Thr$^{410/403}$) were used. After removal of the original signals, we carried out Western blot analysis of β-actin on the same membranes as loading controls for each PKC isoform as described under "Experimental Procedures." Since the patterns of protein bands of β-actin for all 5 isoforms were similarly detected, we present the results of β-actin on phospho-PKC(pan) as a representative at the *bottom* of the lanes.

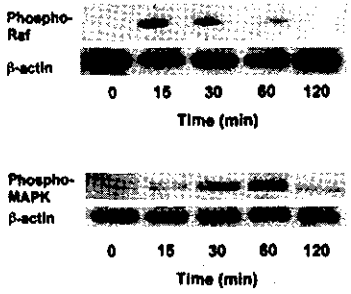

FIG. 9. **Phosphorylation of Raf and MAPK in response to MIF.** Dermal fibroblasts were stimulated for the indicated time intervals (0–120 min) by MIF (100 ng/ml). Western blot analysis was performed on whole cell lysates (40 μg) and antibodies against phospho-Raf, and anti-phospho-p44/p42-MAPK were used. Western blot analysis for β-actin is shown as a control.

Effects of Protein Kinase Inhibitors on PKC and MAPK Activation by MIF—To assess the involvement of tyrosine kinase on PKC and MAPK activation in dermal fibroblasts, we examined whether these inhibitors suppressed the phosphorylation of PKCα/βII and MAPK in response to MIF (100 ng/ml) at 60 min. tyrosine kinase inhibitors, including PP2, genistein, and herbimycin A, were found to suppress PKCα/βII phosphorylation induced by MIF (Fig. 10*a*). Furthermore, we demonstrated that genistein, herbimycin A and PKC inhibitor GF109203X suppressed the phosphorylation of MAPK (Fig. 10*b*).

Effects of CSK on MIF-induced Phosphorylation of PKC and MAPK—Among nonreceptor tyrosine kinases, Src family tyrosine kinases have been reported to activate MAPK (21). We examined the role of Src family tyrosine kinases in MIF-induced phosphorylation of PKC and MAPK using a negative regulator, CSK. We transfected a CSK gene-containing plasmid into cultured dermal fibroblasts and examined the phosphoryl-

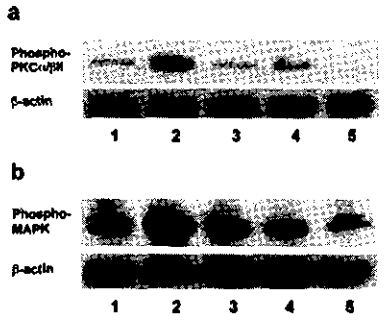

FIG. 10. **Effects of inhibitors on MIF-induced phosphorylation of PKC and MAPK.** Phosphorylation of PKCα/βII and MAPK in dermal fibroblasts induced by MIF was examined in the presence of various inhibitors against PKC and tyrosine kinases. *a*, MIF-induced PKC phosphorylation was measured at 60 min in the presence or absence of tyrosine kinase inhibitors, PP2, genistein, and herbimycin A. Western blot analysis of the cell lysates (40 μg) was carried out using a phospho-PKCα/βII antibody. *Lane 1*, control; *lane 2*, MIF 100 ng/ml; *lane 3*, MIF 100 ng/ml + PP2 10 μM; *lane 4*, MIF 100 ng/ml + genistein 100 μM; *lane 5*, MIF 100 ng/ml + herbimycin A 10 μM. Western blot analysis for β-actin is shown as a control. *b*, MIF-induced MAPK phosphorylation was evaluated at 60 min in the presence or absence of tyrosine kinase inhibitors (genistein, herbimycin A), and PKC inhibitor GF109203X. *Lane 1*, control; *lane 2*, MIF 100 ng/ml; *lane 3*, MIF 100 ng/ml + genistein 100 μM; *lane 4*, MIF 100 ng/ml + herbimycin A 10 μM; *lane 5*, MIF 100 ng/ml +GF109203X 10 μM. Western blot analysis for β-actin is shown as a control.

ation of PKC and MAPK induced by MIF (100 ng/ml) for 60 min. We found that the MIF-induced increase in the phosphorylation of PKC and MAPK was suppressed by transfection of CSK plasmid, whereas CSK^- plasmid had no significant effect (Fig. 11).

DNA Binding Activity of AP-1 in Response to MIF—By using the AP-1 consensus oligonucleotide, the DNA binding activities of AP-1 were examined after MIF stimulation (100 ng/ml). The DNA binding activities of AP-1 were significantly up-regulated for up to 120 min. The binding activity was significantly down-regulated with the addition of an excessive amount of non-labeled AP-1 oligonucleotide (100-fold) (Fig. 12).

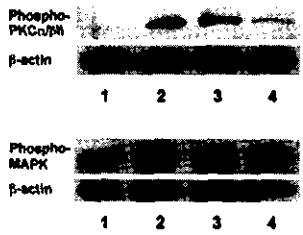

FIG. 11. **Effects of CSK and CSK^- on MIF-induced phosphorylation of PKC and MAPK.** Phosphorylation of PKCα/βII and MAPK in dermal fibroblasts by MIF for 60 min was examined by transfection of CSK and CSK^- plasmid. Western blot analysis of the cell lysates (40 μg) was carried out using phospho-PKCα/βII and phosphoMAPK antibodies. *Lane 1*, control; *lane 2*, MIF 100 ng/ml; *lane 3*, MIF 100 ng/ml +CSK^-, *lane 4*, MIF 100 ng/ml+ CSK. We performed Western blot analysis for β-actin as a control.

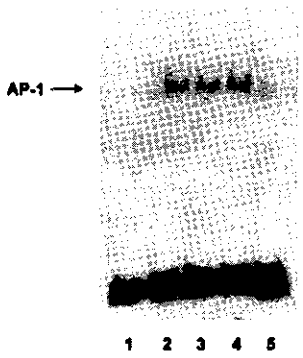

FIG. 12. **EMSA of AP-1 binding activity by MIF stimulation.** Dermal fibroblasts were stimulated with MIF (100 ng/ml) at the indicated times. Nuclear extracts were prepared, and the AP-1 DNA-binding activity was analyzed by EMSA. *Lane 1*, free probe labeled AP-1 binding oligonucleotide without nuclear extracts; *lane 2*, MIF at 0 min; *lane 3*, MIF at 60 min; *lane 4*, MIF at 120 min; *lane 5*, cold AP-1 oligonucleotide (100-fold excess).

DISCUSSION

The effects of sunlight have fascinated researchers for decades because nearly every living organism on earth is likely to be exposed to sunlight, including its ultraviolet (UV) fraction it. Among sunlight's detrimental long term effects is skin photoaging, which is a well-documented consequence of exposure to UVA and UVB radiation. Photoaged skin is biochemically characterized by a predominance of abnormal elastic fibers in the dermis and by a dramatic decrease in distinct collagen types. MMPs are crucial factors involved in the connective tissue remodeling accompanying ultraviolet radiation-induced skin damage.

MIF functions as a pleiotropic cytokine by participating in inflammation and immune responses. MIF was originally discovered as a lymphokine involved in delayed hypersensitivity and various macrophage functions, including phagocytosis, spreading, and cell growth activity (22–24). MIF was recently reevaluated as a proinflammatory cytokine and pituitary-derived hormone that potentiates endotoxemia (25). This protein is ubiquitously expressed in various organs, including the skin, brain, and kidney (27–33). In the skin, MIF is expressed in the epidermis, particularly in the basal layer (15).

Premature aging of the skin secondary to chronic exposure to UV radiation is primarily due to qualitative and quantitative changes in the dermal extracellular matrix, resulting in increased fragility, reduced recoil capacity, blister formation, and impaired wound healing. Interstitial collagens, the major structural components of the dermis, have been found to be particularly diminished in actinically damaged skin. Although there is a direct role for human dermal fibroblasts and an indirect participation of epidermal keratinocytes in MMP-1 production after UVB irradiation, UVA irradiation is known to reach the reticular dermis, rendering fibroblasts possible targets. Recent studies have shown that UV irradiation significantly affects the coordinated regulation of various MMPs and TIMPs (2). The expression of MMPs is regulated at a transcriptional level by various cytokines and other mediators in both a positive and negative manner under certain physiological conditions. Moreover, the enzyme activities of MMPs are post-transcriptionally controlled by activation of latent proenzymes as well as by interactions with their specific inhibitors, referred to as TIMPs.

It has been reported that the biosynthesis of MMP-1 is up-regulated by 12-*O*-tetradecanoylphorbol-13-acetate (TPA), cytokines, and growth factors such as IL-1, TNF-α, IL-6, epidermal growth factor, and platelet-derived growth factor, in a variety of cells, including fibroblasts. In contrast, transforming growth factor-β, retinoic acid, and dexamethasone down-regulate MMP-1 (34). We have recently demonstrated that MIF expression is significantly up-regulated by growth factors such as TGF-β and PDGF (35). These findings indicate that the mRNA of metalloproteinases may be precisely regulated through a complex mechanism that includes both growth factors and cytokines. UVA irradiation of human dermal fibroblasts was found to elicit an increase in specific quantities of mRNA and the bioactivities of the cytokines IL-1α and IL-1β; it

then induced interrelated IL-1 autocrine feedback loops, ultimately leading to tissue degradation in photoaging. Singlet oxygen is an early intermediate in the signaling pathway of IL-1-mediating UVA induction of interstitial collagenase. IL-1α and IL-1β may, at least in part, cause the imbalance between MMPs and TIMPs. For example, there have been reports that the generation of singlet oxygen and other reactive oxygen species precedes the induction of IL-1 (36).

We have here demonstrated that UVA stimulation leads to a significant increase in specific MIF mRNA and protein levels in human dermal fibroblasts. This remarkable increase in MIF occurred by UVA irradiation at intensities above 2 J/cm^2. We also found that IL-1α and IL-1β up-regulate MIF (data not shown). Furthermore, it was found that MIF has the potential to stimulate IL-1β production. Constitutive collagenase synthesis has been reported to be regulated by an IL-1β autocrine mechanism (36). In this study, we demonstrated that anti-MIF neutralizing antibody suppresses the expression of MMP-1 induced by UVA. It is therefore possible that UVA irradiation may stimulate MIF production by an autocrine loop of both MIF and IL-1. MIF up-regulates MMP-1 mRNA as well as protein levels and MMP-1 activity by zymography in dermal fibroblasts. In contrast, TIMP-1 is slightly up-regulated by MIF.

In the present study, we also demonstrated that protein expression of MMP-13 is significantly decreased compared with the levels in control WT-mice after UVA irradiation (10 J/cm^2). In the rodent, regulation of MMP-13 most likely plays an important role in extracellular matrix degradation. These results indicate that MIF-deficient skin especially fibroblasts produce less MMP-13 after UVA irradiation. We therefore hypothesize that MIF participates in the production of MMP-13 and is a significant factor in the degradation of the extracellular matrix in the dermis.

The molecular mechanisms of UV-induced MMPs have yet to be defined. UV-induced expression of pro-inflammatory cytokines such as IL-1β and TNF-α may also in part account for the expression of MMPs. IL-1β-induced expression of MMP-1 is mediated by transactivation of the EGF receptor and through an ERK pathway in human keratinocytes. Collagenase synthesis by fibroblasts and keratinocytes involves the PKC second-messenger system, and corticosteroids have been shown to suppress its synthesis at the level of gene transcription. Long-wavelength UV light (UVA, 320–400 nm) stimulates the synthesis of interstitial collagenase and increases PKC activity in human skin fibroblasts *in vitro*. Ultraviolet irradiation activates growth factor and cytokine receptors on keratinocytes and dermal cells, resulting in downstream signal transduction through an activation of MAP kinase pathways. These signaling pathways converge in the nucleus of cells to induce c-Jun, which heterodimerizes with the constitutively expressed c-Fos to form activated complexes of the transcription factor AP-1. In the dermis and epidermis, AP-1 induces the expression of the matrix metalloproteinases, such as collagenase, 92-kDa gelatinase, and stromelysin, which degrade collagen and other proteins that comprise the dermal extracellular matrix. It has been reported that MIF induces MMP-1 via tyrosine kinase-, PKC-, and AP-1-dependent pathways in synovial fibroblasts in patients with rheumatoid arthritis (34). Consistent with this finding, we showed that the DNA binding activity of AP-1 was up-regulated by MIF stimulation. Furthermore, a JNK inhibitor blocks the activation of c-Jun and has no effect on p38 and MAPK activities (37, 38). In the present study, we observed a reduction in the MMP-1 mRNA level using a specific JNK inhibitor. Therefore, it is conceivable that activation of c-Jun plays an important role in the signal transduction pathway of MIF-induced MMP-1 expression.

Furthermore, we demonstrated that protein kinase C, raf, and MAPK were phosphorylated, but p38 was not phosphorylated in the same manner. Activation of PKC is one of the earliest events in the cascade leading to a variety of cellular responses. There are multiple PKC isoforms, including classical PKCs (α, βI, βII, and γ), which bind calcium, diacylglycerol (DAG) and phospholipids; novel PKCs (δ, ϵ, η, and θ), which are regulated by DAG and phospholipids; and atypical PKCs: ζ and λ, which lack calcium- or DAG-binding domains. Human dermal fibroblasts are known to express α, δ, ϵ, and ζ isoforms of PKC. Among them, PKCα is thought to be the dominant isoform in the fibroblasts (26). By MIF stimulation, we showed the phosphorylation of PKCα/βII and δ occurred, but not that of PKCζ/λ, suggesting that activation of PKCα or δ can play an important role in MIF signal transduction. CSK has been reported to phosphorylate the carboxyl tyrosine residues of Src family tyrosine kinases and inhibit their functions (17). Using CSK and a kinase-negative mutant of CSK (CSK$^-$) in addition to chemical inhibitors, phosphorylation of PKC and MAPK by MIF stimulation was suppressed by CSK, genistein, and herbimycin A. These facts strongly suggest that PKC and MAPK activation depends on activation of Src family tyrosine kinases.

In conclusion, MIF was found to be up-regulated by UVA irradiation in association with IL-1 in human dermal fibroblasts. Upon MIF stimulation, PKC, Raf, and MAPK can be activated in dermal fibroblasts, and up-regulation of the DNA-binding activity of AP-1 might also take place. Clinically, it has been reported that MIF is closely related to the exacerbation of a variety of diseases, including autoimmune diseases, allergic disease, and carcinogenesis. Hence, this newly identified mechanism may contribute to our understanding of photo-induced dermal connective tissue damage, which results in photoaging. These findings are promising for the potential of MIF inhibitors for therapeutic use in patients with severe photodamage related disorders.

Acknowledgment—We thank Ayumi Honda for technical assistance.

REFERENCES

1. Ohnishi, Y., Tajima, S., Akiyama, M., Ishibashi, A., Kobayashi, R., and Horii, I. (2000) *Arch. Dermatol. Res.* **292**, 27–31
2. Fisher, G. J., Wang, Z. Q., Datta, S. C., Varani, J., Kang, S., and Voorhees, J. J. (1997) *N. Engl. J. Med.* **337**, 1419–1428
3. Brenneisen, P., Oh, J., Wlaschek, M., Wenk, J., Briviba, K., Hommel, C., Herrmann, G., Sies, H., and Scharffetter-Kochanek, K. (1996) *Photochem. Photobiol.* **64**, 877–885
4. Brauchle, M., Gluck, D., Di Padova, F., Han, J., and Gram, H. (2000) *Exp. Cell Res.* **258**, 135–144
5. Alexander, J. P., and Acott, T. S. (2001) *Invest. Ophthalmol. Vis. Sci.* **42**, 2831–2838
6. Wlaschek, M., Heinen, G., Poswig, A., Schwarz, A., Krieg, T., and Scharffetter-Kochanek, K. (1994) *Photochem. Photobiol.* **59**, 550–556
7. Rutter, J. L., Benbow, U., Coon, C. I., and Brinckerhoff, C. E. (1997) *J. Cell. Biochem.* **66**, 322–336
8. Kawaguchi, Y., Tanaka, H., Okada, T., Konishi, H., Takahashi, M., Ito, M., and Asai, J. (1996) *Arch. Dermatol. Res.* **288**, 39–44
9. David, J. R. (1966) *Proc. Natl. Acad. Sci. U. S. A.* **56**, 72–77
10. Bloom, B. R., and Bennett, B. (1966) *Science* **153**, 80–82
11. Nishihira, J. (1998) *Int. J. Mol. Med.* **2**, 17–28
12. Bucala, R. (1996) *FASEB J.* **10**, 1607–1613
13. Nishihira, J. (2000) *J. Interferon. Cytokine. Res.* **20**, 751–762
14. Herrmann, G., Wlaschek, M., Lange, T. S., Prenzel, K., Goerz, G., and Scharffetter-Kochanek, K. (1993) *Exp. Dermatol.* **2**, 92–97
15. Shimizu, T., Ohkawara, A., Nishihira, J., and Sakamoto, W. (1996) *FEBS Lett.* **381**, 199–202
16. Nishihira, J., Kuriyama, T., Sakai, M., Nishi, S., Ohki, S., and Hikichi, K. (1995) *Biochim. Biophys. Acta* **1247**, 159–162
17. Sabe H., Hata A., Okada M., Nakagawa H., Hanafusa H. (1994) *Proc. Natl. Acad. Sci. U. S. A.* **91**, 3984–3988
18. Honma, N., Koseki, H., Akasaka, T., Nakayama, T., Taniguchi, M., Serizawa, I., Akahori, H., Osawa, M., and Mikayama, T. (2000) *Immunology* **100**, 84–90
19. Shimizu, T., Abe, R., Ohkawara, A., Mizue, Y., and Nishihira, J. (1997) *Biocem. Biophys. Res. Commun.* **240**, 173–178
20. Yu, W., Woessner, F., Jr. (2001) *Anal. Biochem.* **293**, 38–42
21. Cano, E., Mahadevan, L. (1995) *Trends Biochem. Sci.* **20**, 117–122
22. Adachi, O., Kawai, T., Takeda, K., Matsumoto, M., Tsutsui, H., Sakagami, M.,

Nakanishi, K., and Akira, S. (1998) *Immunity* **9,** 143–150
23. Nathan, C. F., Karnovsky, M. L., and David, J. R. (1971) *J. Exp. Med.* **133,** 1356–1376
24. Churchill, W. H., Jr., Piessens, W. F., Sulis, C. A., and David, J. R. (1975) *J. Immunol.* **115,** 781–786
25. Nishino, T., Bernhagen, J., Shiiki, H., Calandra, T., Dohi, K., and Bucala, R. (1995) *Mol. Med.* **1,** 781–788
26. Choi, S. W., Park, H. Y., Rubeiz, N. G., Sachs, D., and Gilchrest, B. A. (1998) *J. Dermatol. Sci.* **18,** 54–63
27. Suzuki, T., Ogata, A., Tashiro, K., Nagashima, K., Tamura, M., and Nishihira, J. (1999) *Brain. Res.* **816,** 457–462
28. Lan, H. Y., Yang, N., Brown, F. G., Isbel, N. M., Nikolic-Paterson, D. J., Mu, W., Metz, C. N., Bacher, M., Atkins, R. C., and Bucala, R. (1998) *Transplantation* **66,** 1465–1471
29. Lan, H. Y., Mu, W., Yang, N., Meinhardt, A., Nikolic-Paterson, D. J., Ng, Y. Y., Bacher, M., Atkins, R. C., and Bucala, R. (1996) *Am. J. Pathol.* **149,** 1119–1127
30. Imamura, K., Nishihira, J., Suzuki, M., Yasuda, K., Sasaki, S., Kusunoki, Y., Tochimaru, H., and Takekoshi, Y. (1996) *Biochem. Mol. Biol. Int.* **40,** 1233–1242
31. Tesch, G. H., Nikolic-Paterson, D. J., Metz, C. N., Mu, W., Bacher, M., Bucala, R., Atkins, R. C., and Lan, H. Y. (1998) *J. Am. Soc. Nephrol.* **9,** 417–424
32. Bacher, M., Meinhardt, A., Lan, H. Y., Dhabhar, F. S., Mu, W., Metz, C. N., Chesney, J. A., Gemsa, D., Donnelly, T., Atkins, R. C., and Bucala, R. (1998) *Mol. Med.* **4,** 217–230
33. Nishibori, M., Nakaya, N., Tahara, A., Kawabata, M., Mori, S., and Saeki, K. (1996) *Neurosci. Lett.* **213,** 193–196
34. Onodera, S., Kaneda, K., Mizue, Y., Koyama, Y., Fujinaga, M., and Nishihira, J. (2000) *J. Biol. Chem.* **275,** 444–450
35. Takahashi N., Nishihira J., Sato Y., Kondo M., Ogawa H., Ohshima T., Une Y., and Todo S. (1998) *Mol. Med.* **4,** 707–714
36. Wlaschek, M., Wenk, J., Brenneisen, P., Briviba, K., Schwarz, A., Sies, H., and Scharffetter-Kochanek, K. (1997) *FEBS Lett.* **413,** 239–242
37. Bonny, C., Oberson, A., Negri, S., Sauser, C., and Schorderet, D. F. (2001) *Diabetes* **50,** 77–82
38. Bennett, B. L., Sasaki, D. T., Murray, B. W., O'Leary, E. C., Sakata, S. T., Xu, W., Leisten, J. C., Motiwala, A., Pierce, S., Satoh, Y., Bhagwat, S. S., Manning, A. M., and Anderson, D. W. (2001) *Proc. Natl. Acad. Sci. U. S. A.* **98,** 13681–13686

See related Commentary on page v

Novel ALDH3A2 Heterozygous Mutations Are Associated with Defective Lamellar Granule Formation in a Japanese Family of Sjögren–Larsson Syndrome

To the Editor:

Sjögren–Larsson syndrome (SLS: MIM# 270200) is an autosomal recessive disorder characterized by congenital ichthyosis, mental retardation, and spastic paresis (Rizzo, 1993). Rizzo *et al* (1988) demonstrated that long-chain fatty alcohol was deposited in cultured fibroblasts, white blood cells, and serum in SLS patients. Later, De Laurenzi *et al* (1996) reported that mutations in the fatty aldehyde dehydrogenase (FALDH) gene (ALDH3A2) were responsible for the development of SLS. However, the exact pathomechanisms of this ichthyosis in SLS is not fully understood. In this study, we report novel heterozygous mutations in ALDH3A2 in a Japanese family with SLS. In this family, a combination of heterozygous mutations is associated with defective lamellar granules and abnormal intercellular lipid in the stratum corneum.

Case 1: A 6-year-old girl with congenital ichthyosis, mental retardation, and spastic paresis in both her lower extremities, visited our clinic (Fig 1*A*). Physical examination revealed xerosis and fine scales over her whole body, and lamellar-shaped scales on her dorsal hands and feet. Her lower extremities were hypertonic. Brain magnetic resonance imaging (MRI) demonstrated a high-intensity area in the postangular area of the left parietal lobe. Ophthalmologic examination was unremarkable.

Case 2: A 1-year-old boy, the younger brother of case 1, was brought to our clinic suffering from congenital ichthyosis, mental retardation, and spastic paresis on both his lower extremities. Physical examination revealed brown-colored pigmentation with mild to moderate hyperkeratosis on his neck, with fine, dark scales on the dorsal feet (Fig 1*B*). No other abnormalities, including ophthalmologic problems, were observed.

To elucidate the genetic abnormality of the patients, blood samples were collected from both patients and their parents. All the experiments, skin biopsies and blood sampling were performed with the parents' written informed consent and with the institutional approval of Hokkaido University Graduate School of Medicine for experiments handling human matter in accordance with Helsinki Principles. The ALDH3A2 gene was amplified by the methods previously reported by Rizzo *et al* (1999). DNA sequencing of all the PCR products was carried out using a Genetic Analyzer 310A automatic sequencer (Perkin-Elmer Life Sciences-ABI, Foster City, California). In both children, we detected a combination of heterozygous mutations in exon 4 and 7 (Fig 1C). The mutation in exon 4 (481delA) was only present in their mother, and the mutation in exon 7

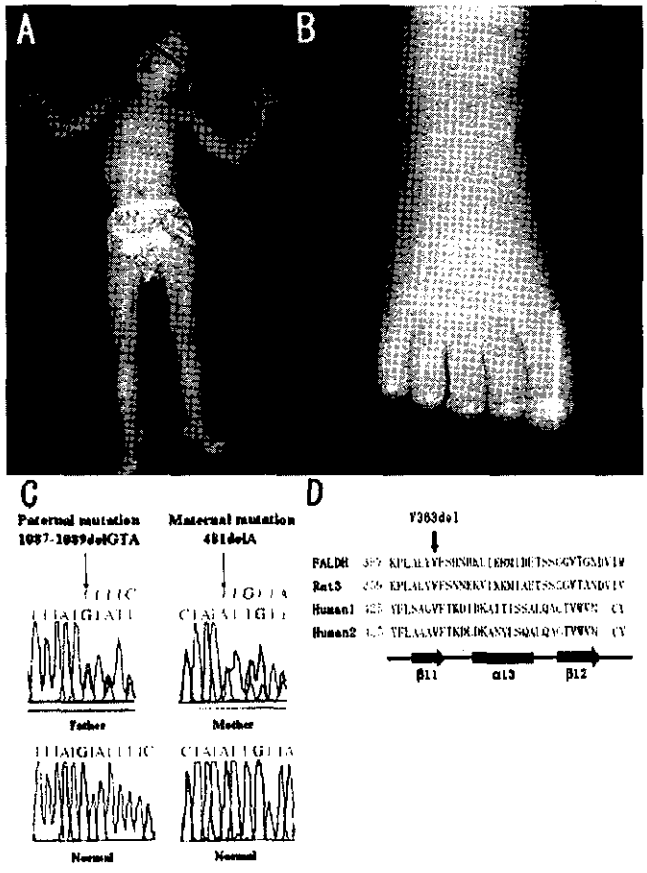

Figure 1
Clinical features and fatty aldehyde dehydrogenase (FALDH) gene (ALDH3A2) mutations. (*A*) Low magnification clinical view of case 1. Xerotic skin and fine scales over the entire body and spastic paresis on both lower extremities. (*B*) High magnification clinical view of case 2. Fine gray scales present on the dorsal feet. (*C*) Sequence analysis of the ALDH3A2. A combination of heterozygous mutations derived from their mother (481delA in exon 4) and father (1087–1089delGTA in exon 7) were detected. (*D*) A sequence alignment between the FALDH, rat class 3 and human class 1 and class 2 ALDH showing the relative locations of key residues in these enzymes. Strictly conserved residues are highlighted in red, while highly conserved residues are shown in blue. Secondary structure components found in the class 3 rat ALDH structure are presented in blue, bars represent α-helices and arrows represent β-strands. (Modified from the paper by Liu *et al*, 1997.)

Abbreviations: ALDH, aldehyde dehydrogenase; FALDH, fatty aldehyde dehydrogenase; SLS, Sjögren–Larsson syndrome

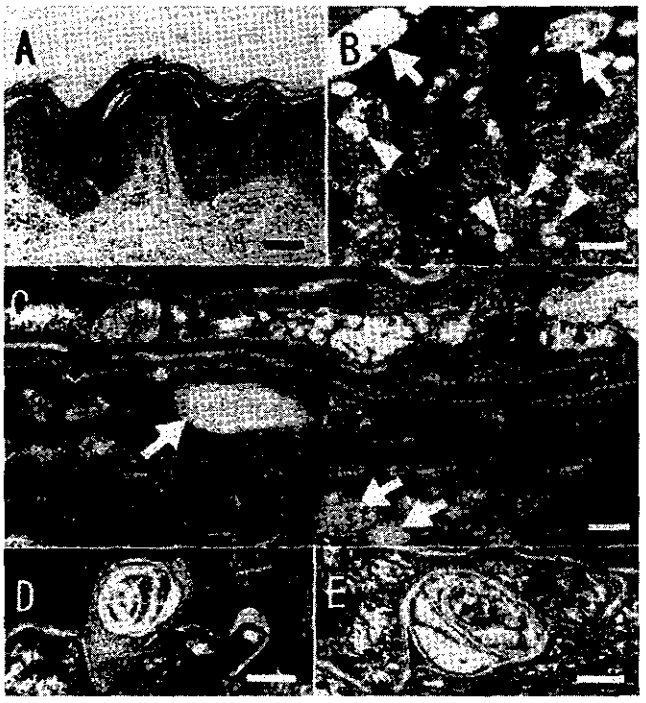

Figure 2
Morphological features of the patient's epidermis. (*A*) Histopathology of ichthyotic skin lesion of case 1. Orthohyperkeratosis with mild hypergranulosis was observed. (*B*) Ultrastructurally, at the stratum granulosum/stratum corneum interface, abnormal apparently empty lamellar granules (*white arrowheads*) were seen in the granular cells and lipid vacuoles (*white arrows*) were observed in the cornified cells. (*C–E*) Vacuoles, presumably lipid droplets (*white arrows*) and irregularly shaped abnormal intercellular materials (*black arrows*) were apparent in the stratum corneum layers. Scale bars = 50 (*A*) and 0.3 μm (*B–E*).

(1087–1089delGTA) was only demonstrated in their father. The presence of both these mutations was excluded in 100 alleles of 50 normal unrelated Japanese individuals.

Histopathological examination of the skin biopsy specimens obtained from both cases revealed orthohyperkeratosis with mild hypergranulosis (Fig 2*A*). Electron microscopic examination of osmium tetroxide-fixed samples from the lesional skin of both patients, demonstrated the abnormal lamellar granules lacking the normal lamellar contents (Fig 2*B*). Some of the defective lamellar granules secreted their components into the intercellular space in the stratum corneum. Irregularly shaped granular and electron-lucent materials were also deposited in the dilated intercellular space between corneocytes (Fig 2*C–E*). Variously sized empty vacuoles, presumably containing electron lucent lipid, were also seen in the stratum corneum (Fig 2*B*, *C*).

Immunofluorescent staining for keratin 1, 10, loricrin, and involucrin, performed as described previously (Akiyama *et al*, 1998), revealed that all of these molecules were normally distributed in the epidermis (data not shown). The distribution pattern of a *trans*-Golgi network marker, TGN-46 and a lamellar granule component, cathepsin D (Ishida-Yamamoto *et al*, 2004) were normal, although immunofluorescent staining for glucosylceramides revealed an abnormal, irregular or granular distribution of glucosylceramides in the patients' stratum corneum (data not shown).

Normal epidermal transglutaminase activity was confirmed in both patients by the *in situ* transglutaminase activity assays previously described elsewhere (Hohl *et al*, 1998; Raghunath *et al*, 1998; Akiyama *et al*, 2001) (data not shown).

FALDH is a microsomal NAD-dependent enzyme, which is necessary for the oxidation of long-chain aliphatic aldehydes to fatty acids (Kelson *et al*, 1997). Until now, several mutations in ALDH3A2 have been shown to be responsible for SLS around the world (Rizzo *et al*, 1999).

In our cases, a heterozygous combination of two novel mutations has been identified. The maternal mutation 481-delA in exon 4 resulted in a frame-shift leading to a stop codon at codon 522. This premature translation termination eliminates the downstream 64% of ALDH3A2 coding sequences. The paternal mutation 1087–1089delGTA in exon 7 resulted in a deletion of valine at position 363 of FALDH protein. According to a comparison of 145 full-length ALDH-related sequences by Perozich *et al* (1999), this valine is highly conserved among many of the ALDH family members, and participates in one of the ten most conserved sequence motifs in ALDH. In addition, analysis of the crystallized 3-D structure of the related class 3 rat cytosolic ALDH revealed that this valine is located at one of the six parallels of β-strands, β11, comprising the catalytic domain of the molecule (Fig 1*D*) (Liu *et al*, 1997). These findings strongly suggest that valine at position 363 is important for structural folding of the catalytic domain and are therefore essential for the normal function of the FALDH protein.

Previously, abnormal lamellar or membranous inclusions in the cornified cells were observed in the lesional skin of a SLS patient, although causative genetic abnormalities were not known in that particular case (Ito *et al*, 1991). The inclusions were speculated to be lamellar granule-in-origin. Later, a deficiency in acyl-ceramides in the lipid layer in the stratum corneum was also reported in SLS patients (Paige *et al*, 1994). In addition to these previous observations, we revealed that the malformed lamellar granule components were secreted into the intercellular space, and irregular-shaped granular and electron-lucent materials were deposited in the irregularly dilated intercellular space in stratum corneum. Immunofluorescence studies revealed an abnormal distribution of glycosylceramide, a lamellar granule component, in the patients' stratum corneum. These observations together suggest defective lamellar granule formation in these patients.

Similarly, a large number of abnormal lamellar granules associated with disturbed intercellular lamellar structures were observed in ichthyotic skin in a patient with Dorfman–Chanarin syndrome (Akiyama *et al*, 2003). Furthermore, in harlequin ichthyosis, lamellar granules are completely absent or, if present, are not correctly secreted into the intercellular space (Milner *et al*, 1992). Thus, the present ultrastructural and immunofluorescence findings suggest that formation of defective lamellar granule contents and defective intercellular lipids, presumably related to the mutations in ALDH3A2, may lead to the ichthyotic skin developed in SLS patients.

Akihiko Shibaki, Masashi Akiyama, and Hiroshi Shimizu
Department of Dermatology, Hokkaido University Graduate School of Medicine, Sapporo, Japan

This work was supported in part by a grant-in-aid from the Ministry of Education, Culture, Sports, Science and Technology (B16390312 to M. A.).

DOI: 10.1111/j.0022-202X.2004.23505.x

Manuscript received April 20, 2004; revised July 29, 2004; accepted for publication July 29, 2004

Address correspondence to: Akihiko Shibaki, MD, PhD, Hokkaido University Graduate School of Medicine, N 15 W 7, Kita-ku, Sapporo 060-8638, Japan. Email: ashibaki@med.hokudai.ac.jp

References

Akiyama M, Christiano AM, Yoneda K, Shimizu H: Abnormal cornified cell envelope formation in mutilating palmoplantar keratoderma unrelated to epidermal differentiation complex. J Invest Dermatol 111:133–138, 1998

Akiyama M, Sawamura D, Nomura Y, Sugawara M, Shimizu H: Truncation of CGI-58 protein causes malformation of lamellar granules resulting in ichthyosis in Dorfman–Chanarin syndrome. J Invest Dermatol 121:1029–1034, 2003

Akiyama M, Takizawa Y, Suzuki Y, Ishiko A, Matsuo I, Shimizu H: Compound heterozygous TGM1 mutations including a novel missense mutation L204Q in a mild form of lamellar ichthyosis. J Invest Dermatol 116:992–995, 2001

De Laurenzi V, Rogers GR, Hamrock DJ, *et al*: Sjögren–Larsson syndrome is caused by mutations in the fatty aldehyde dehydrogenase gene. Nat Genet 12:52–57, 1996

Hohl D, Aeschlimann D, Huber M: *In vitro* and rapid *in situ* transglutaminase assays for congenital ichthyoses—a comparative study. J Invest Dermatol 110:268–261, 1998

Ishida-Yamamoto A, Simon M, Kishibe M, *et al*: Epidermal lamellar granules transport different cargoes as distinct aggregates. J Invest Dermatol 122:1137–1144, 2004

Ito M, Oguro K, Sato Y: Ultrastructural study of the skin in Sjögren–Larsson syndrome. Arch Dermatol Res 283:141–148, 1991

Kelson TL, Secor McVoy JR, Rizzo WB: Human liver fatty aldehyde dehydrogenase: Microsomal localization, purification, and biochemical characterization. Biochim Biophys Acta 1335:99–110, 1997

Liu Z-J, Sun Y-J, Rose J, *et al*: The first structure of an aldehyde dehydrogenase reveals novel interactions between NAD and the Rossmann fold. Nat Struct Biol 4:317–326, 1997

Milner ME, O'Guin WM, Holbrook KA, Dale BA: Abnormal lamellar granules in harlequin ichthyosis. J Invest Dermatol 99:824–829, 1992

Paige DG, Morse-Fisher N, Harper JI: Quantification of stratum corneum ceramides and lipid envelope ceramides in the hereditary ichthyoses. Br J Dermatol 131:23–27, 1994

Perozich J, Nicholas H, Wang B-C, Lindahl R, Hempel J: Relationships within the aldehyde dehydrogenase extended family. Protein Sci 8:137–146, 1999

Raghunath M, Hennies HC, Velten F, Wiebe V, Steinert PM, Reis A, Traupe H: A novel *in situ* method for the detection of deficient transglutaminase activity in the skin. Arch Dermatol Res 290:621–627, 1998

Rizzo WB: Sjögren–Larsson syndrome. Semin Dermatol 2:210–218, 1993

Rizzo WB, Carney G, Lin Z: The molecular basis of Sjögren–Larsson syndrome: Mutation analysis of the fatty aldehyde dehydrogenase gene. Am J Hum Genet 65:1547–1560, 1999

Rizzo WB, Dammann AL, Craft DA: Sjögren–Larsson syndrome. Impaired fatty alcohol oxidation in cultured fibroblasts due to deficient fatty alcohol: Nicotinamide adenine dinucleotide oxidoreductase activity. J Clin Invest 81:737–744, 1988

Characterization of Kdap, a Protein Secreted by Keratinocytes

Shuichi Tsuchida,*[1] Makoto Bonkobara,*[2] James R. McMillan,† Masashi Akiyama,† Tatsuo Yudate,*‡ Yoshinori Aragane,‡ Tadashi Tezuka,‡ Hiroshi Shimizu,† Ponciano D. Cruz Jr,* and Kiyoshi Ariizumi*

*Department of Dermatology, The University of Texas Southwestern Medical Center, and the Dallas Veterans Affairs Medical Center, Dallas, Texas, USA; †Department of Dermatology, Hokkaido University Graduate School of Medicine, Sapporo, Japan; ‡Department of Dermatology, Kinki University School of Medicine, Osaka, Japan

Using a signal sequence-trap we identified a human gene encoding a polypeptide of 99 amino acids with a putative signal sequence. The gene was identical to keratinocyte differentiation-associated protein (Kdap), which was reported previously by Oomizu *et al* (Gene 256: 19–27, 2000) to be expressed in embryonal rat epidermis at the mRNA level. In humans, we found Kdap mRNA expression to be restricted to epithelial tissue at high levels. The 12.5 kDa protein was detected in culture supernatant of keratinocytes and those transfected adenovirally with the Kdap gene. In normal skin, Kdap protein was found exclusively within lamellar granules of granular keratinocytes and in the intercellular space of the stratum corneum. By contrast, in lesional skin of patients with psoriasis, Kdap was expressed more widely throughout suprabasal keratinocytes. When induced to differentiate *in vitro*, keratinocytes showed marked upregulation of Kdap mRNA expression similar to that of involucrin mRNA, but with differing kinetics. Finally, a spliced variant of Kdap mRNA was generated by alternative splicing mechanisms. Our studies indicate that human Kdap resembles rat Kdap with respect to tissue and cell expression at the mRNA level and that Kdap is a low-molecular-weight protein secreted by keratinocytes. Thus Kdap may serve as a soluble regulator of keratinocyte differentiation.

Key words: alternative splicing/cDNA cloning/differentiation/keratinocyte/secreted protein
J Invest Dermatol 122:1225–1234, 2004

As the outermost layer of skin, the epidermis serves as an interface between internal and external environments. It consists overwhelmingly of keratinocytes, which originate from stem cells and transiently amplifying cells in the basal layers, which in turn proliferate and differentiate first into spinous keratinocytes and then into granular keratinocytes (Watt, 2000). The latter cells' distal outer and inner cell membranes correspond, respectively, to lipid and protein envelopes that together form the cornified cell envelope (CCE). The protein envelope consists of an insoluble complex of proteins cross-linked by transglutaminase (TGase) to structural proteins such as involucrin and loricrin, whereas the lipid envelope consists of a monomolecular layer of ω-hydroxyceramides, covalently linked by ester bonds to the protein envelope (Kalinin *et al*, 2001).

The CCE a mechanical barrier that can forestall entry through the skin of infectious microbes, mutagenic ultraviolet radiation, noxious chemicals, and other injurious agents. Recent studies also suggest that it may play an active role in innate immunity. Molecular cloning and protein analyses have identified several secreted proteins of low molecular weight within the CCE (e.g., SKALP/elafin; cystatins) (Steinert and Marekov, 1995; Ishida-yamamoto and Iizuka, 1998; Schalkwijk *et al*, 1999), and functional studies have shown that many of these proteins exert proteinase inhibitor activity that may curtail microbial growth and/or dampen inflammation (Molhuizen and Schalkwijk, 1995).

Despite recent recognition of CCE components and elucidation of their functions, it is likely that several important components of the CCE remain undiscovered. The identification and elucidation of their function should improve our understanding of CCE. Hypothesizing that some of these novel CCE proteins are secreted and keratinocyte-specific proteins (e.g., involucrin, filagrin, and loricrin), we employed a previously established signal sequence (SS)-trap method (Tashiro *et al*, 1993) to isolate SS-coding genes from a human keratinocyte cDNA library because the N-terminal SS is unique to precursors of secreted and membrane-anchored proteins. SS-trapped cDNA clones were then screened for keratinocyte-specific genes using differential colony hybridization (keratinocytes *vs* dermal fibroblasts). Our efforts yielded several novel genes including one encoding a precursor of a secreted, low-molecular-weight protein expressed selectively in normal human epidermis by granular keratinocytes. Subsequent analyses have revealed the gene to be identical to keratinocyte differentiation-associated protein (Kdap), isolated by Oomizu *et al* (2000).

Oomizu *et al* identified Kdap using subtractive cDNA cloning of rat embryo skin at 14 *vs* 17 d of gestation. They

Abbreviations: CCE, cornified cell envelope; Kdap, keratinocyte differentiation-associated protein; PBS, phosphate-buffered saline

[1]Present address: Department of Biology, University of Nippon Veterinary and Animal Science, Tokyo, Japan.

[2]Present address: Department of Veterinary Clinical Pathology, University of Nippon Veterinary and Animal Science, Tokyo, Japan.